RESEARCH AND DEVELOPMENT TECHNICAL REPORT

DELNV-TR-79-5

DEVELOPMENT OF THE NEODYMIUM PENTAPHOSPHATE (NPP) LASER

J. Gualtieri
NIGHT VISION & ELECTRO-OPTICS LABORATORY

October 1979

ERADCOM

US ARMY ELECTRONICS RESEARCH & DEVELOPMENT COMMAND
FORT MONMOUTH, NEW JERSEY 07703

NOTICES

Disclaimers

The citation of trade names and names of manufacturers in
this report is not to be construed as official Government
indorsement or approval of commercial products or services
referenced herein.

Disposition

Destroy this report when it is no longer needed. Do not
return it to the originator.

REPORT DOCUMENTATION PAGE		READ INSTRUCTIONS BEFORE COMPLETING FORM
1. REPORT NUMBER DELNV-TR-79-5	2. GOVT ACCESSION NO.	3. RECIPIENT'S CATALOG NUMBER
4. TITLE *(and Subtitle)* DEVELOPMENT OF THE NEODYMIUM PENTAPHOSPHATE (NPP) LASER		5. TYPE OF REPORT & PERIOD COVERED Final Tech Report
		6. PERFORMING ORG. REPORT NUMBER
7. AUTHOR(s) J. Gualtieri		8. CONTRACT OR GRANT NUMBER(s)
9. PERFORMING ORGANIZATION NAME AND ADDRESS US Army ERADCOM ATTN: DELNV-L Fort Monmouth, NJ 07703		10. PROGRAM ELEMENT, PROJECT, TASK AREA & WORK UNIT NUMBERS 61102A 1T161102AH46 E1 021C8
11. CONTROLLING OFFICE NAME AND ADDRESS US Army ERADCOM ATTN: DELNV-L Fort Monmouth, NJ 07703		12. REPORT DATE October 1979
		13. NUMBER OF PAGES 47
14. MONITORING AGENCY NAME & ADDRESS(if different from Controlling Office)		15. SECURITY CLASS. *(of this report)* Unclassified
		15a. DECLASSIFICATION/DOWNGRADING SCHEDULE

16. DISTRIBUTION STATEMENT *(of this Report)*

Unlimited; Approved for Public Release.

17. DISTRIBUTION STATEMENT *(of the abstract entered in Block 20, if different from Report)*

18. SUPPLEMENTARY NOTES

19. KEY WORDS *(Continue on reverse side if necessary and identify by block number)*

Solid state laser materials
Neodymium pentaphosphate
Miniature rangefinder application
Laser considerations
Device considerations

20. ABSTRACT *(Continue on reverse side if necessary and identify by block number)*

The structural properties of NPP are examined and the effect of twin domain boundaries on light propagation are discussed. Spectroscopic properties of NPP and other lanthanide pentaphosphates are outlined. The advantages of NPP as a laser material for miniature rangefinder and long distance fiber optic application are discussed. Laser and device considerations are reviewed and a miniature NPP laser cavity with all components individually removable for easy replacement (overall size 1.5 x 1.5 x 4.4 cm)

DD FORM 1473 EDITION OF 1 NOV 65 IS OBSOLETE
1 JAN 73

1

are discussed.

TABLE OF CONTENTS

5 14

5

DEVELOPMENT OF THE NEODYMIUM PENTAPHOSPHATE (NPP) LASER

INTRODUCTION

Late in 1972, the announcement of intense infrared emission in the compound NdP_5O_{14}, as opposed to ordinary Nd doped solid state laser materials such as Nd:YAG, aroused much interest in the laser community.[1] The significance of this for Army/DOD laser applications was clearly recognized, and shortly thereafter, a small group of investigators was assembled at ERADCOM, NV&EO Laboratories, Fort Monmouth to study the growth and optical properties of this new type of laser material. For about two years, laser research on these materials was confined to the study of as-grown crystals almost microscopic in size. In 1975, significant results were achieved regarding the preparation and laser performance of large (4.5 x 3 x 2.2 mm) perfect optical quality NdP_5O_{14} crystals. However, the impact on future Army laser rangefinders and designators could not be evaluated until the growth of larger crystals was established. Thus, the in-house developed technology was transferred to industry (Philips Laboratories) for the development of 10 mm long laser rods. Contractor performance was excellent and the technology was advanced to provide laser rods up to 20 mm in length. In addition, through an ARO funded contract, concurrent studies were performed at Lincoln Laboratories to examine resonator effects and thermal properties of flashlamp pumped mini-lasers. Laser performance was significantly improved as a result of this work.

ADVANTAGES OF PENTAPHOSPHATES

The lanthanide pentaphosphates are hard, stable crystalline materials which may be inexpensively grown to a high degree of perfection and optical quality. They make excellent hosts for the lanthanide series of rare-earth ions.

NPP is a high optical gain laser material, mainly as a result of a 30 X increase in concentration over ordinary Nd lasers. (In Figure 1 the absorption coefficient for both NPP and Nd:YAG are plotted as a function of wavelength.) There is little fluorescence quenching, lifetime reduction or linewidth broadening and no optical degradation of the material with increasing concentration. These unique properties of NPP have been suggested as resulting from: (a) The large Nd-Nd separation of 0.52 nm which reduces Nd^{+3} dipole-dipole interactions. In YAG the Nd-Nd separation can be as small as 0.37 nm.[1]

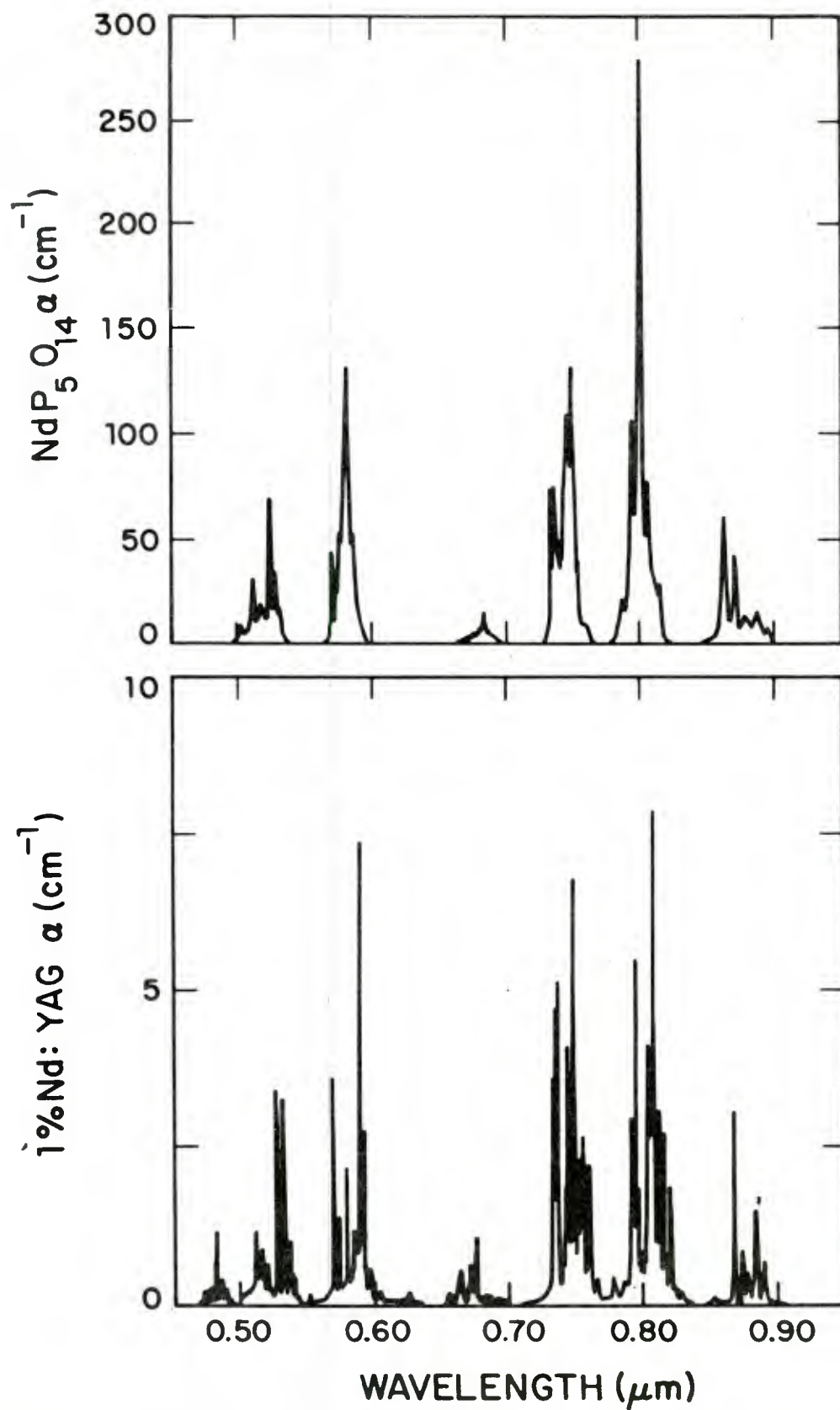1. H. G. Danielmeyer and Heinz P. Weber, IEEE Jour. Quant. Elect. QE-8, 805 (1972).

Figure 1. Absorption coefficient as a function of wavelength for Nd:YAG and NPP.

(b) A favorable position of the $^4I_{15/2}$ manifold relative to the upper laser manifold ($^4F_{3/2}$) and the ground manifold ($^4I_{9/2}$). This reduced cross-relaxation between Nd ions.[2] (c) The fact that the Nd-0 polyhedra are unconnected in NPP. This isolation affects the cross-relaxation quenching mechanism both by increasing the Nd-Nd separation and modifying the crystal-field splitting of the $^4I_{15/2}$ manifold.[3]

In projecting the use of NPP, several possible advantages over existing materials are apparent. The Nd concentration can be varied over the full (0-100%) range by dilution with inert cations such as La or Y. This allows a "molecular engineering" of the chemical composition to obtain a specific pump band absorption strength. Uniform pumping and increased absorption by the lasing medium is of prime importance since the efficiency of the laser is related to the amount of pump radiation absorbed. This means that one can "tailor" the material for low threshold or high output power for CW, pulsed or Q-switched operation. The high degree of polarization of the NPP laser output, which is a consequence of its inherent gain anisotropy, will also facilitate electro-optic Q-switching. The potential military benefit for a rangefinder/designator application is in providing a low cost, miniature, low threshold,high efficiency laser transmitter. Additional advantages of NPP vs LED's or injection lasers for long distance high data rate fiber optic communications systems are: Better operating service lifetimes, better mode control and beam divergence, lower spectral waveguide dispersion (narrower linewidth), higher output power with transverse pumping. The current status and limitations of injection lasers and NPP type lasers for use in future long distance fiber optic communications systems are outlined in Table 1.

GROWTH AND STRUCTURAL PROPERTIES

The growth of bulk crystals of NPP at ERADCOM and under ERADCOM sponsorship has been adequately covered in previous reports.[4-6]

2. H. G. Danielmeyer, M. Blatte and P. Balmer, Appl. Phys. 1, 269 (1973).

3. H. Y-P Hong, Acta. Cryst. B30 (1974).

4. A. Schwartz, M. J. Wade, T. R. Aucoin and J. G. Gualtieri, Proc., US Army Science Conference (June 1976).

5. T. R. AuCoin, A. Schwartz, M. J. Wade and J. G. Gualtieri, ECOM R&D Technical Report 4467 (February 1977).

6. W. Zwicker, "Development of Neodymium Pentaphosphate Laser Rods," Report DELNV-TR-77-2154-F, April 1978.

Table 1. Injection lasers versus neodymium pentaphosphate mini-lasers for long distance fiber optic communications applications.

Characteristics	Injection Laser Type		Nd-Pentaphosphate Laser Type	
Emission wavelengths (μm) Both in low loss and dispersion regions of silica fiber	1.06	1.28	1.05	1.32
Emission bandwidth ($\overset{o}{A}$) NPP would have less dispersion-meaning higher information rates	20		1	
Mode Control	Possible, but with substantial power reduction		Relatively easy to obtain	
Power Output	High radiance laser required which may limit device life-time		Power output is scalable through transverse pumping with LED's which have long lifetime. NPP lifetime should be unlimited.	
Modulation capability	Drive current modulation possible to 2 gigahertz		Electro-optic modulation required. 800 MHz demonstrated in miniature $LiNbO_3$ device	
Costs	The cost of injection lasers and their associated modulation equipment should be lower		Advantages of high power, increased life-time, and favorable emission characteristics may compensate for increased costs	

9

a. Structural Properties

The lanthanide pentaphosphates crystallize in three different space groups depending on lanthanide ion radius. The elements La through Tb form a monoclinic structure (pseudo orthorhombic) whose atomic positions allow a smooth transition into orthorhombic symmetry with increasing temperature. The monoclinic cell has a $P2_1/c$ space group (commonly called type I or class I). The elements Tb through Lu, Y, Bi form a second monoclinic structure with a C2/c space group (commonly called type II or class II). The pentaphosphates of Dy, Ho, Er and Y also form a third structure, truly orthorhombic, having space group Pnma (commonly called type III or class III).

The monoclinic type I structure shows a pseudo-orthorhombic symmetry characteristic of space group Pncm. Only very small shifts in atomic position are required to produce a true orthorhombic symmetry. The shifts required for structure reorientation increase as the ionic radii decrease from La through Tb. This reorientation can be introduced abruptly (mechanically) or smoothly (thermally). In type I NPP crystals, two types of twin planes have been found which undergo elastic reorientation through twin boundary motion.[7-8] One observes that twin boundaries can be induced and moved across and out of crystals with very small applied stress. However, their removal is temporary, in that they are reintroduced by similar small stresses, for example, in subsequent handling and fabrication procedures. It was suggested that by choosing an appropriate average ionic radius, mixed crystals containing any of the lanthanide ions could yield any of the three structure types. Since the type III orthorhombic structure pentaphosphates do not exhibit twinning, we would like to have a crystal with the maximum concentration of Nd attainable in type III structure. Using the ionic radius of Tb as indicative of monoclinic type I structure, we can simply require the average ionic radius to be less than 0.94 A.U. Tb has an ionic radius of .93 A.U. and can exist in type II structure. For Y (.92 A.U.) and Nd (1.04 A.U.) the composition for type III structure would be $Nd_{.167}Y_{.833}P_5O_{14}$.

Besides Y we might choose Yb (.86 A.U.) Sc (.81 A.U.) or In (.81 A.U.) as possible diluent ions. Yb can be ruled out for Nd laser purposes since Nd is known to transfer energy to Yb. Sc and In have ionic radii too small to form mixed crystals with Nd except in monoclinic type I structure this has been verified for Sc[9] and by our own growth experiments for In. Unfortunately, the growth of large bulk crystals of diluted NPP

7. H. P. Weber, B. C. Tofield and P. F. Liao, Phys. Rev. B, 11, No. 3, 1st Series 1152 (1975).

8. J. P. Budin, A. Milatos-Roufos, Nguyen Duc Chinh, and G. LeRous, Jour. Appl. Phys. 46, 2867 (1975).

9. H. G. Danielmeyer, G. Huber, W. W. Kruhler and J. P. Jeser, Appl. Phys. 2, 335 (1973).

compounds is difficult. Thus far, only small crystals have been produced which sometimes represented different phases. Large crystals of $Nd_{.5}La_{.5}P_5O_{14}$ have been grown but these were highly strained due to lattice mismatch.[6] Domain free $Nd_{.14}Y_{.86}P_5O_{.4}$ epitaxial layers have been grown on $Gd_{.33}Y_{.67}P_5O_{14}$ substrates. Room temperature CW lasing was reported, with thresholds in the milliwatt range for longitudinal pumping with an argon laser.[10]

b. Twin Boundary Iridescence

It is known that potassium chlorate and calcite occasionally crystallize in twinned forms which display iridescent effects.[11-12] The phenomena of iridescence is generally described as the result of interference of light produced by thin films or by liquid filled cracks in crystals. In twinned crystals, iridescence is a consequence of the anisotropy of the medium and the different orientation of adjacent domains. Light propagating through these crystals is both reflected and refracted at the planes of twinning. Effects such as deviated images exhibiting spectral dispersion and polarization characteristics are easily observed. The index ellipsoids in adjacent domains in NPP have a common axis which coincides with the b axis of the crystal. The iridescent phenomena results because one of the ellipsoids is rotated clockwise (θ = 9.45°) and the other counter-clockwise by the same amount (see Figure 2). Figure 3 is a diagram showing how a single beam of light incident on a crystal plate containing a twin boundary is resolved into 8-beams. Two of the beams in reflection and 2 in refraction at the twin boundary are unresolved and leave the plate unpolarized (indicated by the letter U). Thus, the emergence of two triplets is noted. As the angle of incidence θ is increased to approximately 12-degrees, the vertically polarized components grazing the twin boundary disappear. These components also exhibit spectral dispersion. The effects disappear and laser performance is unaffected when light propagates parallel or perpendicular to the twin plane.[13] The perpendicular direction is the c-axis of the crystal and is the logical choice for the laser resonator direction. Polishing is limited by the presence of elastic twins perpendicular to the c-axis which produces surface irregularities on a faces.

10. W. W. Krühler, R. D. Plättner, W. Fabian, P. Mockel and J. G.Grabmaier, Opt. Comm. 20, 354 (1977).

11. C. V. Raman and A. K. Ramdas, Proc. Ind. Acad. Sci., A40 1 (1954).

12. C. V. Raman and D. Krishnamurti, Proc. Ind. Acad. Sci., A 36, 315 (1952); A 38 261 (1953).

13. J. G. Gualtieri and T. R. AuCoin, Appl. Phys. Lett 28 189 (1976).
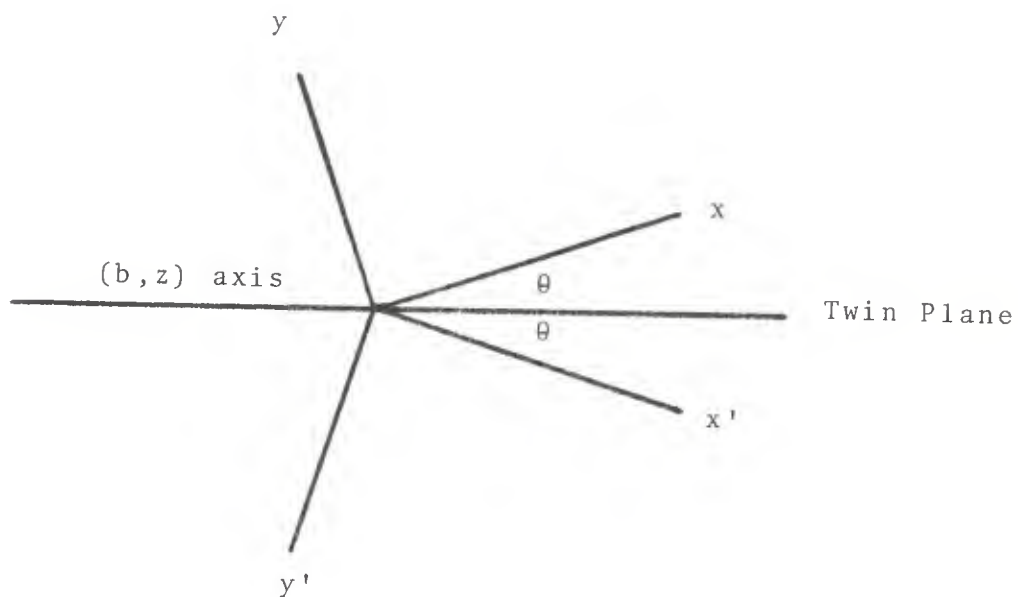
Figure 2.   Orientation of index ellipsoids in adjacent domains
            in NPP. The (b,z) axis is perpendicular to the
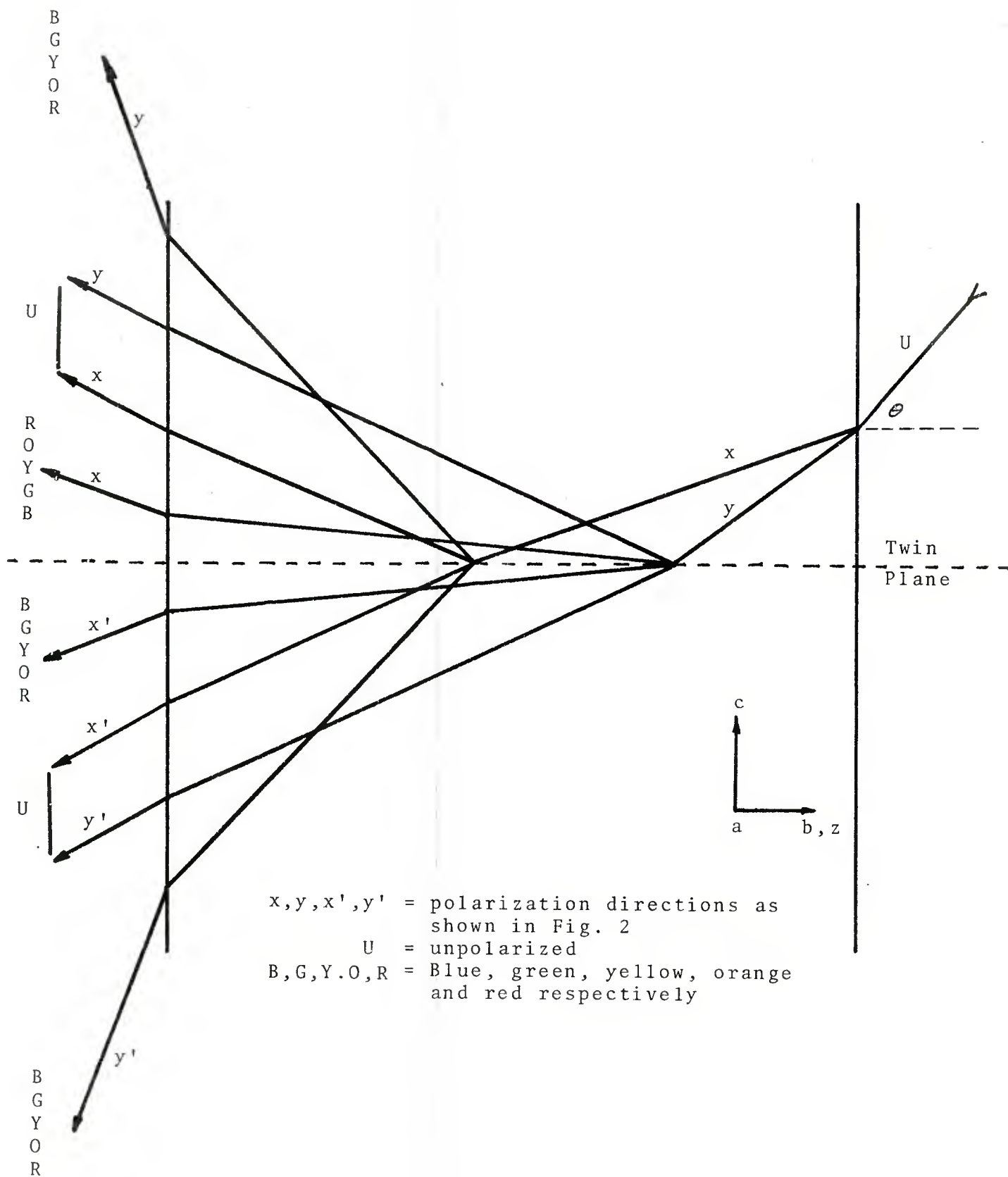   plane of the paper.

Figure 3. Resolution of a single beam of unpolarized
           light into two triplets after reflection and
           refraction at a twin boundary.

13

Polishing is also limited by perfect cleavage parallel to b faces. Fortunately, c-planes can be precision polished.

SPECTROSCOPY

a. Lifetimes and Concentration Quenching

Fluorescence lifetimes corresponding to $^4F_{3/2} \rightarrow {}^4I_{11/2}$ transitions of pentaphosphates of Nd were determined by pulsing samples repetitively with a GaAlAs diode laser (peak wavelength = 810 nm). The resultant fluorescence was filtered and then detected with an RCA 7102 photomultiplier. The repetitive signals were averaged using a boxcar integrator. Lifetimes were determined from the negative slope of the plot of ln I versus time. There is no obvious difference in lifetimes with cooling to 77K. In Table 2 we give the fluorescence lifetimes and Nd concentration for various diluent ions. The lifetimes were found to be sensitive to the growth temperature of the sample. For example, material grown at temperatures below 550°C showed shorter lifetimes possibly as the result of hydroxyl ion trapping within the crystals.

Concentration quenching of the fluorescence was found to be linear in $Nd:LaP_5O_{14}$ while in ordinary Nd doped materials it is usually quadratic. Recently, at our suggestion, the spectroscopic properties of $Nd_xY_{1-x}P_5O_{14}$ have been investigated.[14] It was found that the Nd ions occupy a variety of slightly perturbed sites. No significant energy transfer was found to occur between these ions in inequivalent sites. A new quenching model for NPP based on spatial but non-spectral energy migration to surface quenching sites was suggested. In addition, we have found that it is possible to lengthen the Nd lifetime by about 10% by growing an epitaxial layer of $Gd_{.54}La_{.46}P_5O_{14}$ on a substrate of NPP. This change lends some definite proof to the surface quenching suggestion. Although this increase in lifetime is small, other epilayer compositions and improved growth procedures may lead to increases in lifetime which are helpful technologically.

b. Line Broadening in NPP

The line broadening mechanism in NPP is a temperature dependent effect which does not influence the observed lifetime. For example, the fluorescence lifetime of the $^4F_{3/2} \rightarrow {}^4I_{11/2}$ transition was unchanged when the temperature was lowered from 300°K to 2°K. Moreover, at 300°K, the emission lines are 0.01 nm wide, while at 300°K they are 1.7 nm wide. NPP behaves like a typical thermally broadened material. Physically, thermal

---

14. J. M. Flaherty and R. C. Powell, Phys Rev B 19, No. 1 32 (1979).

Table 2. Advanced laser materials.

Spectroscopic properties of rare-earth pentaphosphates

Element	Fluorescence (μm)	RT Linewidth (A)	RT Lifetime (μs)	Terminal State (cm-1)
Nd	(0.885 (1.052 (1.320	(62 (16 (46	100-300	(200 (2000 (4000
Sm	0.595	60	80	1000
Eu	0.612	9	4800	1000
Tb	0.545	13	4000	2000
Dy	(0.577 (0.488	13 5	342	(3000 (416
Er	1.530	2 @ 77K		131

15

broadening is caused by variations in the crystal field which modulate the energy levels. However, the linewidth changes are not simply proportional to the lattice vibrational amplitude. Dominant lattice vibrations in NPP occur at 450 cm^{-1}, 1000 cm^{-1}, 1170 cm^{-1} and 1300 cm^{-1}. The modulation rate is therefore much greater than the linewidth changes. Higher order interactions are required. For example, two high frequency vibrations may combine to produce a vibration oscillating at the difference frequency. This frequency is then low enough to cause slow variations of the energy of the excited states which can account for the broadening, but do not affect the lifetime. The broadening produced by such a process is homogeneous. From a laser point of view this broadening is not detrimental, since any excited ion in the crystal is free to radiate over the whole lineshape. The probability is greater for emission at the center frequency. Theoretically, emission within the homogeneously broadened envelope will depopulate the upper laser level completely. By contrast an inhomogeneously broadened laser material (e.g. Nd:Glass) is not free to radiate over the entire lineshape, but only over a very narrow wavelength range corresponding to its own spectral packet. For this reason, one saturates or burns holes in the laser gain curve at these center frequencies.

c. Multiphonon Decay

For a given rare-earth ion, the most critical factor affecting the multiphonon relaxation rate is the energy gap to the next lower level. The decay rates exhibit an approximate exponential dependence on energy gap, ΔE, predicted by the equation

$$W = W(o) \, exp \, (-\alpha \, \Delta E)$$

$W(0)$ is the multiphonon transition probability at $T = 0^{\circ}K$ and α is a constant determined by the phonon nature of the host and by the strength of electron lattice coupling. In Table 3 we have indicated the energy gaps below the fluorescing states, the number of high energy (1300 cm^{-1}) phonons required for multiphonon decay in pentaphosphates, and a qualitative fluorescence intensity. From Table 3 we see that ErP_5O_{14} at 5 phonons stands at the limit of room temperature fluorescence. Fluorescence of wavelength longer than 1.54 µm will occur only weakly at room temperature (see section f). Instead, multiphonon decay will dominate and depopulate the excited states. We see from Table 3 that only Nd is a candidate for room temperature infrared pentaphosphate lasers. While for visible lasers Eu, Tb, Dy and Sm pentaphosphate could be considered candidates. ErPP could be considered as a low temperature infrared laser candidate.

16

Table 3. Spectroscopic properties of rare-earth pentaphosphates.

Ion	Largest Energy Gap (cm^{-1} approximately)	No. of 1300 cm^{-1} Phonons required	Room Temperature Fluorescence Intensity
Nd	7,300 *	> 5	Strong (IR)
Sm	7,000	> 5	Distinct (vis)
Eu	12,200	> 9	Strong (vis)
Tb	15,000	> 11	Strong (vis)
Dy	7,000	> 5	Strong (vis)
Ho	5,000	< 4	Very weak (vis)
Er	6,500	5	Weak (IR, vis)
Tm	6,000	< 5	Not detected

* Ignoring the $^4I_{15/2}$ state.

17

d. Crystal Field Symmetry

The absorption and emission spectra corresponding to $^5D_0 \rightarrow {}^7F_J$ transitions of Eu^{3+} yield useful information about its local site symmetry. For example, the transition $^5D_0 \rightarrow {}^7F_0$ corresponds to a J = 0 to J = 0 transition which is strictly forbidden, but if the site symmetry can be described using a linear crystal field term, this transition has a weak but observable intensity. The only site symmetries possessing linear crystal field terms are C_s, C_n and C_{nv}. From the emission of EuP_5O_{14} at $77^{O}K$ (Figure 4), a weak line is observed at 578.5 nm corresponding to a $^5D_0 \rightarrow {}^7F_0$ transition. Also, we observe three lines corresponding to magnetic dipole transitions ($^5D_0 \rightarrow {}^7F_1$) and 5 lines corresponding to $^5D_0 \rightarrow {}^7F_2$. Blanzat, et al[15] originally found only 4 lines for $^5D_0 \rightarrow {}^7F_2$, however, lowering the temperature to $77^{O}K$ reveals a 5th very weak line at 612.5 nm. They reasoned that since the $^5D_0 \rightarrow {}^7F_0$, $^5D_0 \rightarrow {}^7F_1$ and $^5D_0 \rightarrow {}^7F_2$ yielded 1, 3, and 4 lines, respectively, this indicated C_{2v} symmetry. Although they apparently chose the correct symmetry, the existence of the 5th line in $^5D_0 \rightarrow {}^7F_2$ shows that the situation is a bit more complicated. However, since the C_{2v} forbidden 5th line is extremely weak, the effective symmetry to be chosen from spectroscopic consideration is C_{2v}. Thus, we can guess that Nd in the monoclinic I pentaphosphate structure effectively "feels" a C_{2v} symmetry. Later Brecher[16] derived a reasonably complete and consistent picture of the spectroscopic behavior of EuP_5O_{14}. Using polarized emission and absorption spectra of single crystals, he identified most of the observed transitions and derived the energy level structure of the ^7F multiplet. The overall site symmetry was found to be very low (C_1),

15. B. Blanzat, J. P. Denis and J. Loriers, Proc. Tenth Rare-Earth Res. Conf., 2 1170 (1973).

16. C. Brecher, J. Chem. Phys. 61 2297 (1974).

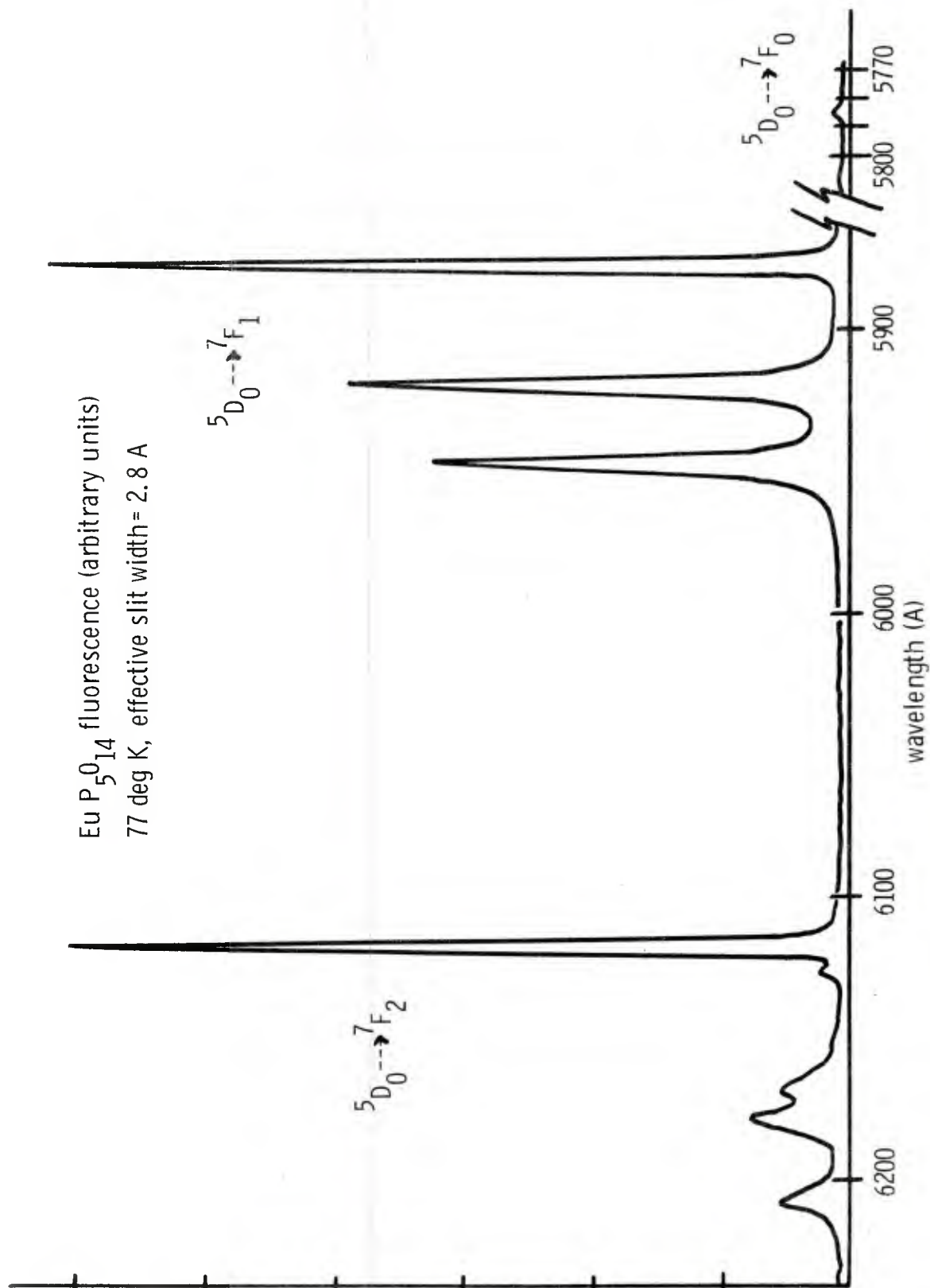Eu P$_5$O$_{14}$ fluorescence (arbitrary units)

77 deg K, effective slit width = 2.8 A

$^5D_0 \longrightarrow {}^7F_0$

$^5D_0 \longrightarrow {}^7F_1$

$^5D_0 \longrightarrow {}^7F_2$

wavelength (A)

Figure 4. Fluorescence spectrum of EuP$_5$O$_{14}$ (77 K).

19

however, the local symmetry of the Eu ion was higher (effectively C_{2v}). The proposed structure of the Eu site was related to a face-centered isoceles prism.

e. Effective Emission Cross-Section

Much has been written concerning stimulated emission cross-sections of Nd:YAG, with values ranging from 1.8×10^{-19} cm^2 to 4.6×10^{-19} cm^2. Original measurements of the cross-section of Nd in NPP were in error by a factor of 2 because of neglect of reabsorption. The following analysis suggested by Weber, et al.[17] may be used to determine the effective emission cross-sections in NPP and Nd:YAG.

The upper laser states for Nd is $^4F_{3/2}$, which is split into two components by the crystal field (upper R_2, lower R_1). In NPP the maximum cross-section $\sigma_{R_1, Y_2} = 1.7 \times 10^{-19}$ cm^2 and corresponds to a $R_1 \rightarrow Y_2$ transition. Y_2 is one of the six crystal field split levels of $^4I_{11/2}$ (the lower laser state). In Nd:YAG the maximum cross section is $\sigma_{R_2, Y_3} = 4.6 \times 10^{-19}$ cm^2. NPP has contributions from two transitions; $\sigma_{R_1, Y_1} = 1.5 \times 10^{-19}$ cm^2 at 1051.3 nm and $\sigma_{R_2, Y_4} = 0.7 \times 10^{-19}$ cm^2 at 1050.6 nm. Their combined contribution is needed to calculate the laser gain. This results in an emission cross section γ, where

$$\gamma = F_{R_1} \sigma_{R_1, Y_1} + F_{R_2} \tilde{\sigma}_{R_2, Y_4}$$

F_{R_i} is the fractional occupation number of the R_ith level of $^4F_{3/2}$. These levels are split 110 cm^{-1} in NPP. Thus,

17. H. P. Weber, P. F. Liao and B. C. Tofield, IEEE J. Quant. Elect. QE-10 563 (1974).

$$F_{R_2} = \frac{N_{R_2}}{N_{R_1} + N_{R_2}} = N_{R_2} = \frac{exp\left(-\frac{110}{kT}\right)}{1 + exp\left(-\frac{110}{kT}\right)}$$

$$F_{R_2} = 0.37 \, , \quad F_{R_1} = 0.63$$

then γ_{NPP} ($R_1 \rightarrow Y_1$, $R_2 \rightarrow Y_4$) = 1.2 x 10^{-19} cm^2. Since the $^4F_{3/2}$ splitting in Nd:YAG is 86 cm^{-1} calculation of F_{R_1} yields 0.602 and F_{R_2} = 0.398 then $\gamma_{Nd:YAG}$ ($R_2 \rightarrow Y_3$) = 1.8 x 10^{-19} cm^2. See Figure 5 for the relevant energy level diagrams.

g. Notes on Lanthanide Ions Other than Nd

1. $Sm_{0.1}Y_{0.9}P_5O_{14}$

To our knowledge, Sm^{3+} has never lased in any host. The fluorescence of this compound compares favorably with that of Sm^{3+}:$CaWO_4$ (see Figure 6). However, the lifetime of the strongest transition at 5945 A.U. is less than 80 μs and the linewidth is very broad (approximately 60 A.U.). The possibility of laser action in this compound is remote.

2. EuP_5O_{14}

Eu^{3+} has lased in Y_2O_3 and YVO_4. The linewidth of the 6122 A.U. emission line in EuP_5O_{14} is approximately 9. A.U., approximately half the width of a similar transition in Y_2O_3 at room temperature. It is known that Tb transfers

21

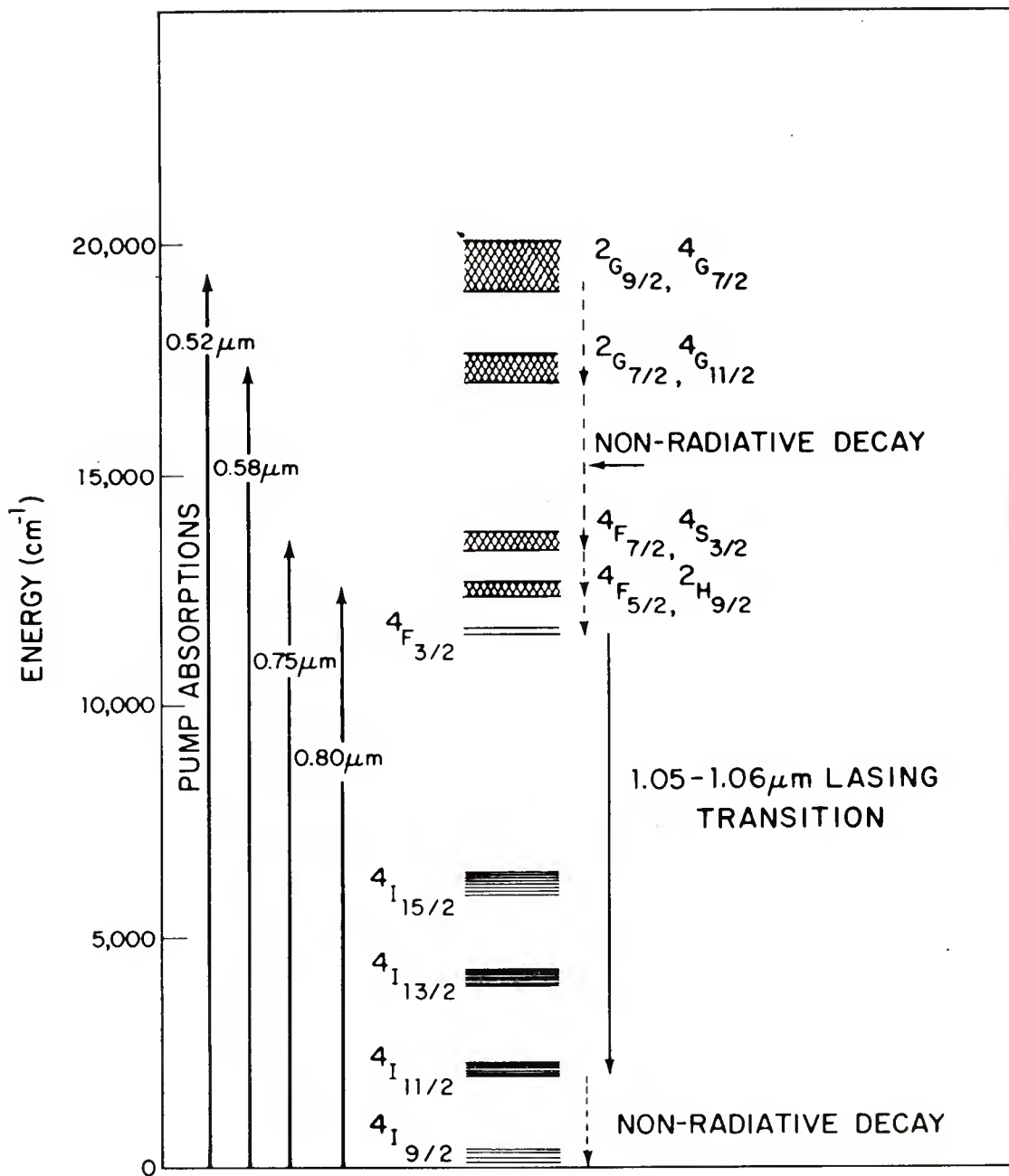Figure 5.   Energy level diagram showing pump absorption, non-radiative decay and principal lasing transitions for the Nd ion.

relative fluorescence (arbitrary units)
300 deg K, effective slit width = 1.6 A

$0.1Sm\ 0.9Y\ P_5O_{14}$ vs Sm : $CaWO_4$

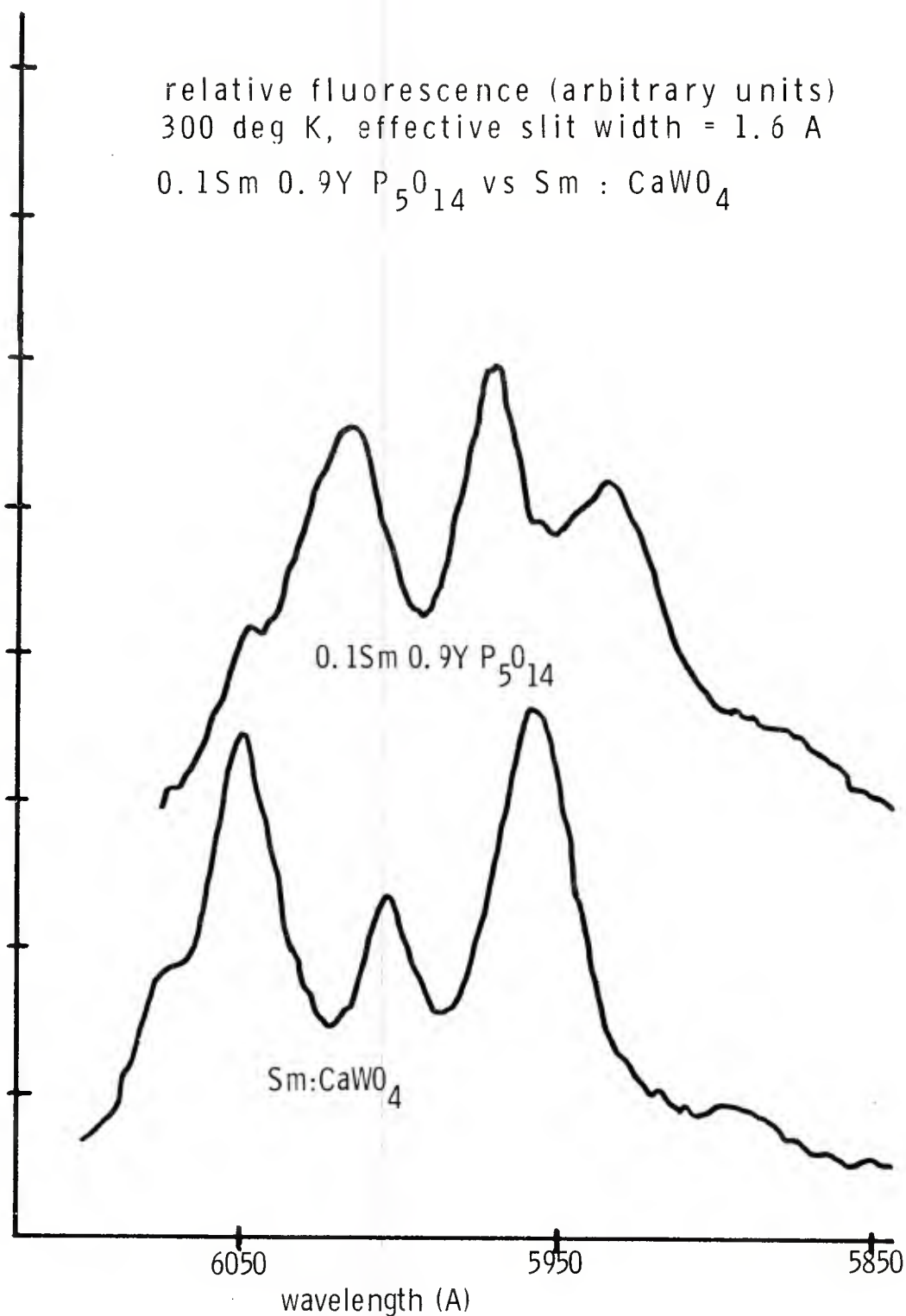$0.1Sm\ 0.9Y\ P_5O_{14}$

Sm:$CaWO_4$

wavelength (A)

Figure 6.   Fluorescence spectrum of samarium pentaphosphate
diluted with yttrium compared to Sm:$CaWO_4$ (300 K).

energy to Eu increasing the initial state population by about 72% in the compound $Eu_{0.2}Tb_{0.8}P_5O_{14}$.[15] The terminal level is approximately 1000 cm^{-1} above ground. See Figure 4 for the relevant fluorescence spectrum.

3. TbP_5O_{14}

A 50 J/in threshold for laser action has been reported for Tb:YLF[18] using the composition $LiY_{0.5}Tb_{0.25}Gd_{0.25}F_4$. The laser transition is within the $^5D_4 \rightarrow {}^7F_5$ multiplet and since $^7F_5$ is 2000 cm^{-1} above ground, this laser operates as a 4 level device. The fluorescence lifetime of 25% Tb in YLF was reported to be approximately 5 ms. TbP_5O_{14} has a fluorescence lifetime of 4 ms for a 5447 A.U. line within the $^5D_4 \rightarrow {}^7F_5$ multiplet the fluorescence spectrum of $Tb_{0.1}Y_{0.9}P_5O_{14}$ is given in Figure 7.

4. $Dy_{0.1}Gd_{0.9}P_5O_{14}$

$Dy_{0.1}Gd_{0.9}P_5O_{14}$ could be a possible laser in the yellow region at 577.4 nm. The transition involved is in the $^4F_{9/2} \rightarrow {}^6H_{13/2}$ emission multiplet. $^6F_{13/2}$ is approximately 3000 cm^{-1} above ground level and the fluorescence lifetime is approximately 340 μs.

Dy^{3+} may also be the only reasonable choice for a blue-green laser for the following reasons: (1) Dy is a good absorber of blue and UV pump radiation. (2) There is an energy gap between the emitting level and the next lower level of at least 5 times the energy of the most energetic lattice phonon available. This means non-radiative relaxation through multiphonon decay is very unlikely. (3) There is no excited state absorption from the initial emitting level to high lying configurations as in the case of terbium. One disadvantage might be that the terminal level is approximately 459 cm^{-1} above ground. Thus, 4-level operation at room temperature is questionable.

We have found the fluorescence of DyP_5O_{14} is quenched, making it necessary to use a composition of only 10% Dy. The choice of either Y or Gd alters the emission spectrum markedly. This is no doubt a result of the structure changes dictated by the differing ionic radii of these ions.

---

18. A. Linz, H. P. Jenssen, D. R. Gabbe, D. Castleberry and M. H. Douma, "Blue-Green Laser Material," Tech. Rept. No. 17, ONR Contract N00014-67-A-0204-044, May 30, 1974.
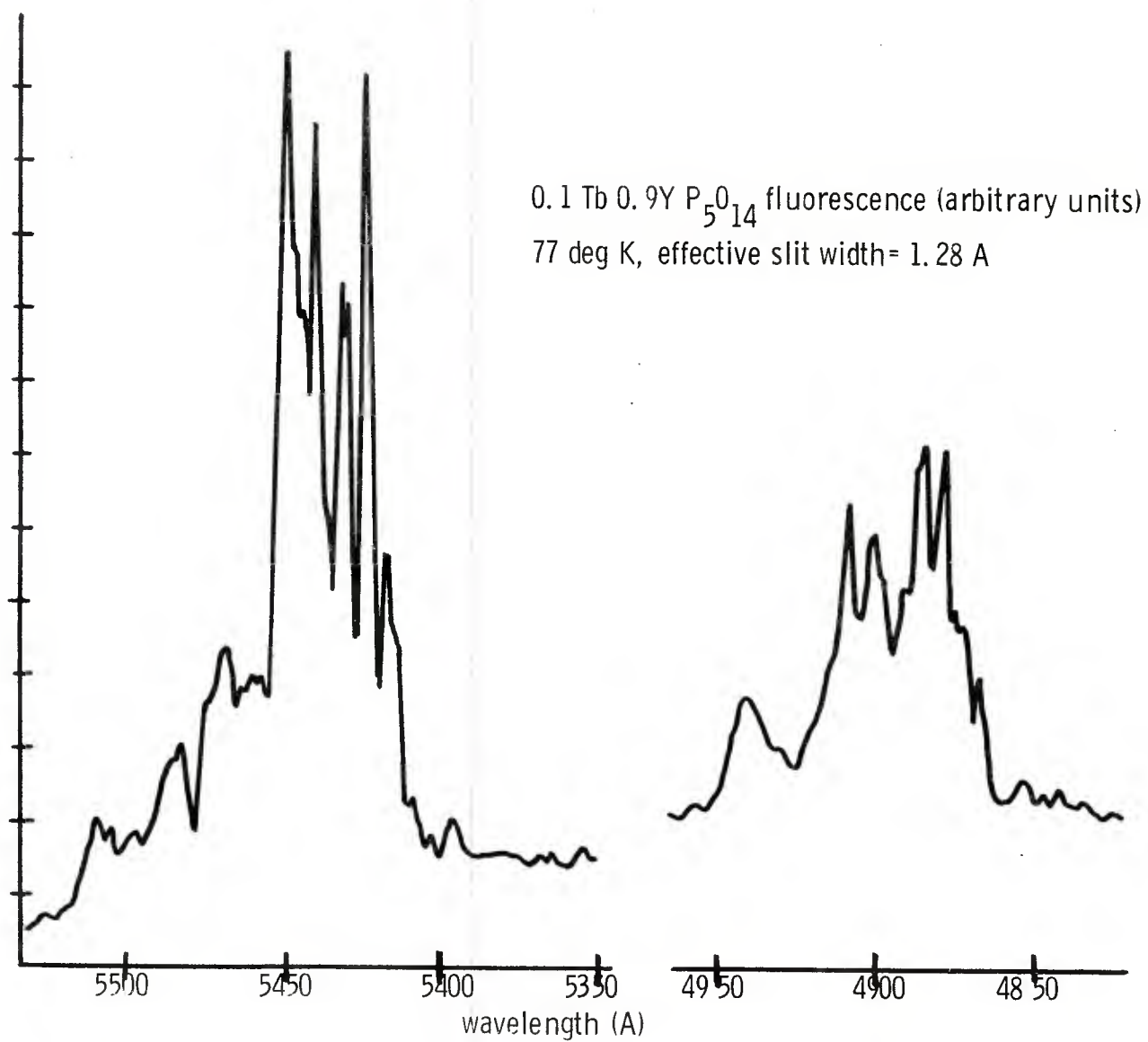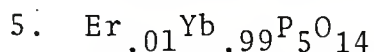
Figure 7.   Fluorescence spectrum of terbium pentaphosphate
diluted with yttrium (77 K).

25

In Figure 8 and Figure 9 we show the fluorescence spectra of these compounds. In the case of the Gd compound, most of the blue-green fluorescence is concentrated in one line at 4879 A.U. The lifetime of this transition was 250 μs.

5. $Er_{.01}Yb_{.99}P_5O_{14}$

The largest energy gap between ^4F levels in Er is between $^4I_{13/2}$ and $^4I_{15/2}$, representing about 5 phonons in the pentaphosphate lattice. Thus, efficient fluorescence and any possible laser action requires cooling the material to at least 77°K. In Figure 10 we show the spectrum of this compound at 77°K.

LASER CONSIDERATIONS

a. Threshold Calculation

The round trip gain exponent should equal the round trip loss at threshold:

$$2 \gamma D_{th} \ell = L_o + L_T$$

where

γ = effective stimulated emission cross section,

ℓ = gain length (usually the crystal length),

L_o = total non-resonant round trip loss including scattering in the laser medium, diffraction and mirror absorption losses.

L_T = round trip transmission loss,

= -ln (product of reflectivities)

then

$$D_{th} = \frac{L_o + L_T}{2 \gamma \ell} = N_{i,th} - N_f = \Delta N_{th}$$

where

N_i,th = number density of ions in the initial laser level at threshold,

N_f = number density of ions in the final laser level.

26

0. 1Dy 0. 9Y P$_5$0$_{14}$ fluorescence (arbitrary units)

effective slit width = 1. 28 A, 300 deg K

attenuation factor = 1

wavelength (A)

Figure 8. Fluorescence spectrum of dysprosium pentaphosphate diluted with yttrium (300 K).

27

0.1Dy 0.9Gd P_5O_{14} fluorescence (arbitrary units)

300 deg K, effective slit width = 1.12 A
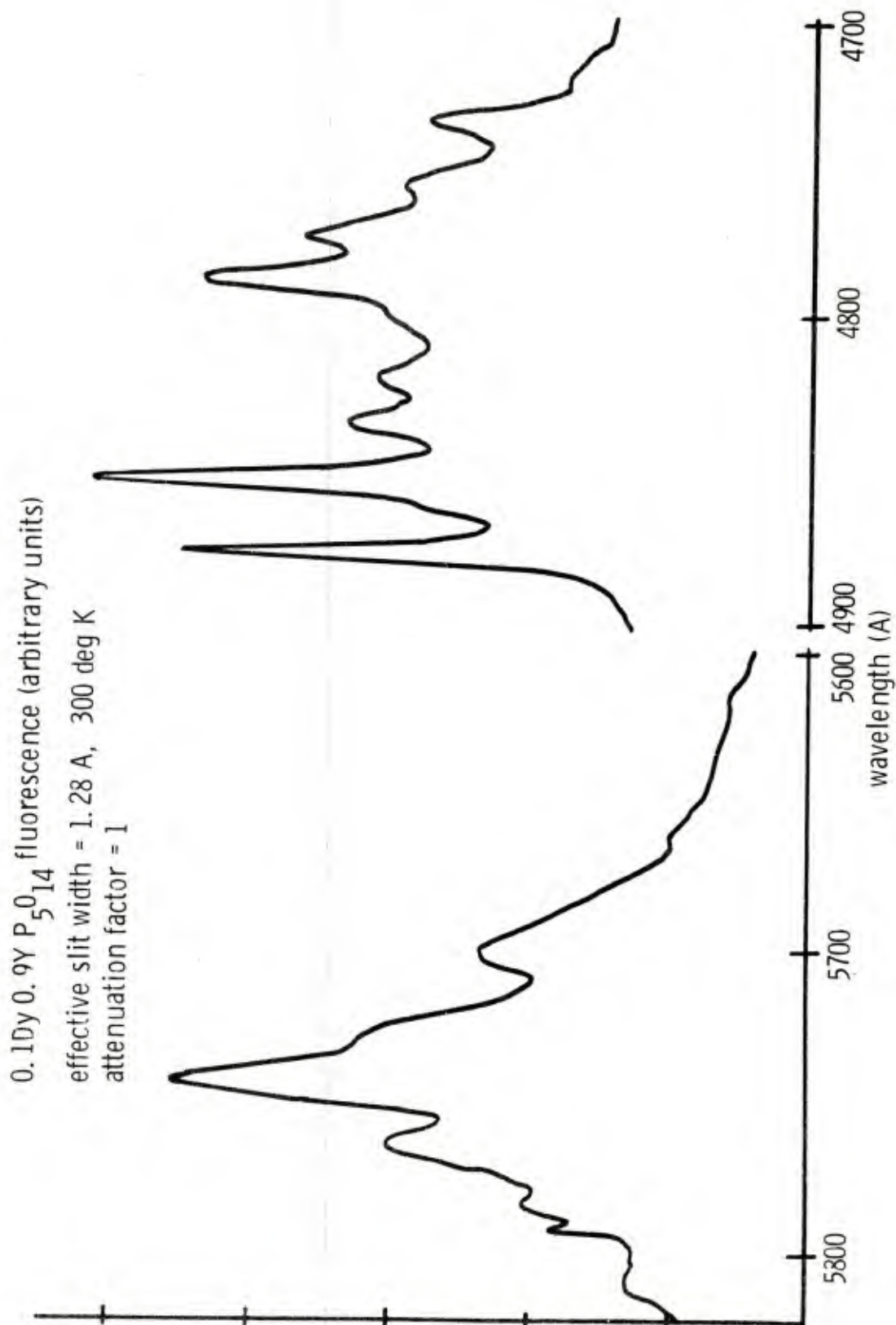attenuation factor = 2

wavelength (A)
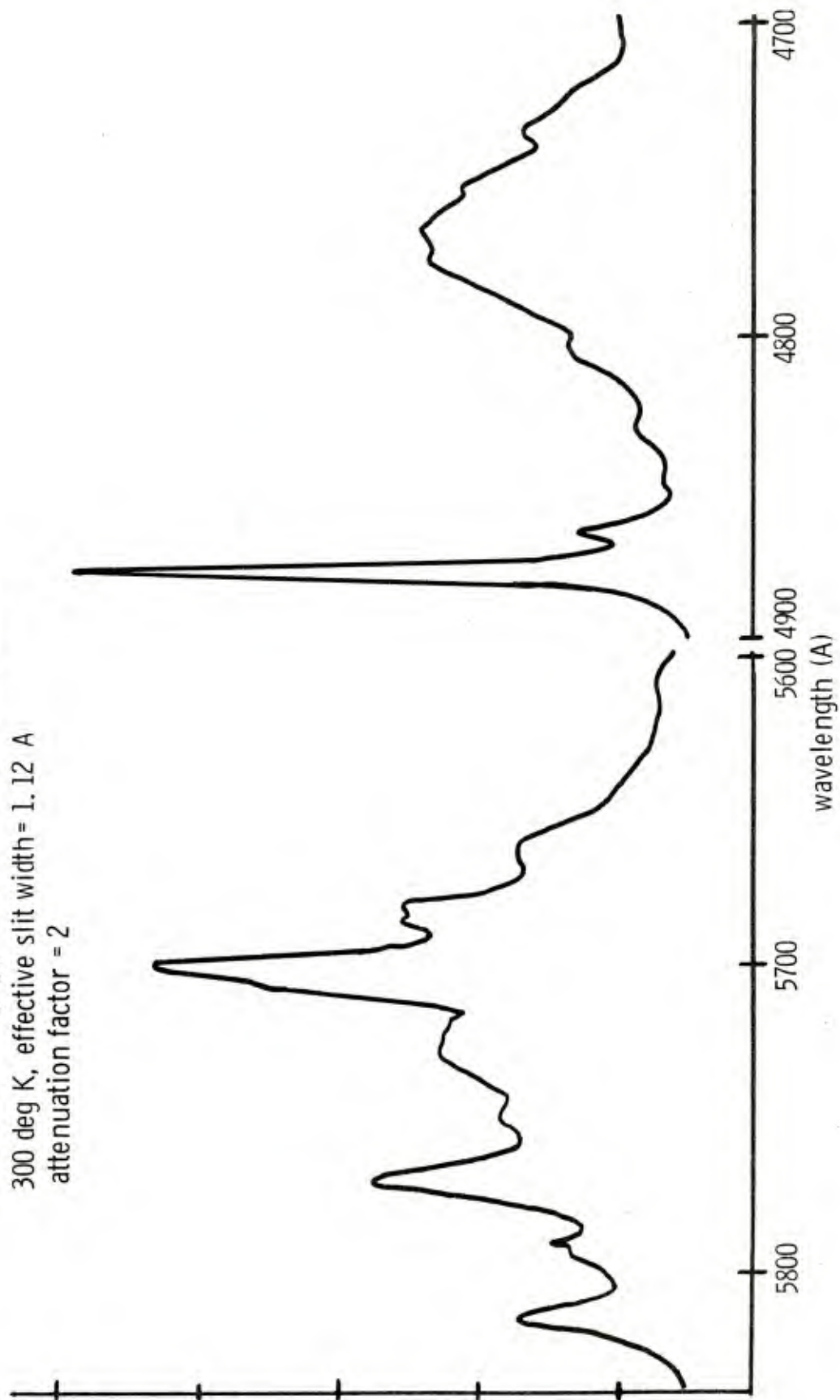
Figure 9. Fluorescence spectrum of dysprosium pentaphosphate diluted with gadolinium (300 K).

0.01Er 0.99Yb P_5O_{14} fluorescence
(arbitrary units) 77 deg K
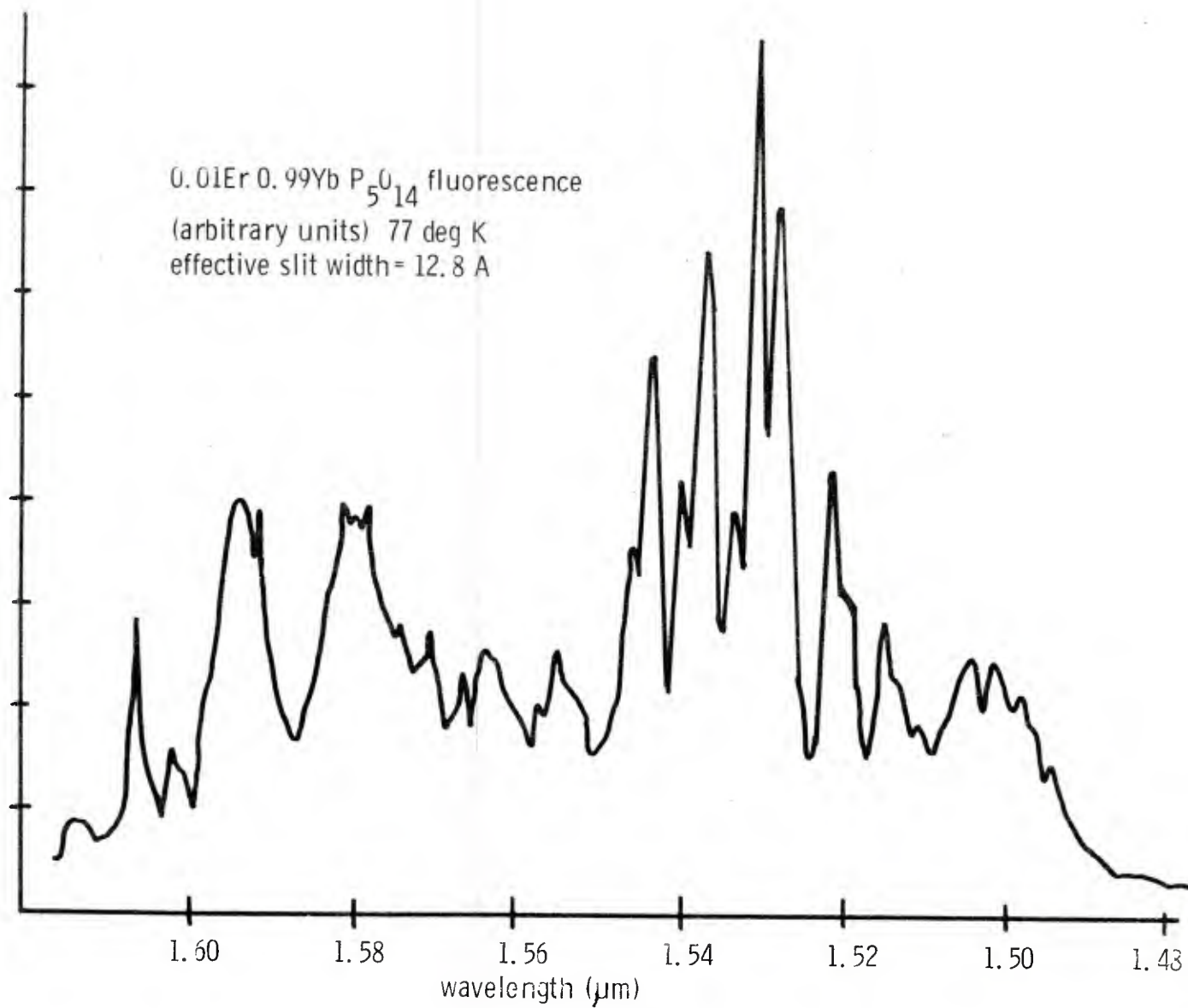effective slit width= 12.8 A

wavelength (μm)

Figure 10.   Fluorescence spectrum of erbium pentaphosphate
diluted with ytterbium (77 K).

The density in the final state is

$$N_f \simeq \frac{N}{Z} \exp\left(-E_f/kT\right)$$

here N is the density of Nd ions in the crystal, Z is the partition function, $z = \sum_j \exp(E_j/kT)$. The density of ions in the initial state may be written as

$$N_{i,th} = \frac{P_{th}\, \tau_f\, \eta_p}{V\, h\nu_p}$$

where P_{th} is defined as the absorbed power at threshold,

η_p is the quantum efficiency for pumping (Ni/No. of pumped ions)

V is the pumped volume,

τ_f is the lifetime of the initial level.

Thus, $Ni_{th} - N_f = \dfrac{P_{th}\, \tau_f\, \eta_p}{V\, h\nu_p} - \dfrac{N}{Z} \exp\left(-E_f/kT\right)$

the absorbed power at threshold is

$$P_{th} = \frac{V\, h\nu_p}{\tau_f\, \eta_p} \left[\frac{L_0 + L_T}{2\gamma\ell} + \frac{N}{Z} \exp\left(-E_f/kT\right) \right]$$

$$P_{th} = \frac{V\, h\nu_p}{\tau_f\, \eta_p} \frac{1}{2\gamma\ell} \left[L_0 + L_T + L_R \right] = P\left[L_0 + L_T + L_R \right] = P[L]$$

where L_R is the round trip resonant loss and $L_R = 2\gamma\ell\, N/Z \quad X$ exp$(-E_f/kT)$.

If we want to obtain the incident pump intensity in Watts/cm^2 necessary to achieve threshold, we must introduce the fraction absorbed. For example, for a square cross section rod of diameter d, length ℓ and absorption coefficient α_p:

$$I(\text{absorbed}) = I(\text{incident}) - I(\text{transmitted})$$

for colinear pumping:
$$I_a = I_i \left(1 - \exp(-\alpha_p \ell)\right),$$

for transverse pumping:
$$I_a = I_i \left(1 - \exp(-\alpha_p d)\right),$$

therefore (I_{th}) colinear becomes:

$$\frac{h\nu_p}{\tau_f \eta_p} \quad \frac{[L]}{2\gamma(1 - \exp(-\alpha_p \ell))}$$

and (I_{th}) transverse =

$$\frac{h\nu_p d}{\tau_f \eta_p} \quad \frac{[L]}{2\gamma\ell(1 - \exp(-\alpha_p d))}$$

In what follows, we would like to compare the NPP laser material with the more thoroughly developed Nd:YAG materials.

If we calculate the ratio (I_{th})NPP/(I_{th})Nd:YAG by assuming colinear pumping using, for example, a GaAlAs LED with ℓ optimized to α_p^{-1} we find that

$$(I_{th})_{NPP} / (I_{th})_{Nd\,YAG} \approx \frac{\tau_{YAG}}{\tau_{NPP}} \quad \frac{\gamma_{YAG}}{\gamma_{NPP}} \approx 3$$

We have used τ_{YAG} = 230 µs and τ_{NPP} = 120 µs in this calculation. The absorption lengths are 9 mm for 1.3% Nd:YAG (the highest practical Nd concentration in Nd:YAG), and only 0.3 mm for NPP. For a similar resonator configuration, this results in a larger mode area on the rod face for Nd:YAG. The mode area

$$\approx \pi \left[w(\ell/2) \right]^2$$

where $W(\frac{\ell}{2})$ is the spot size on the rod face. Assuming a typical fundamental mode waist radius w_o = 30 µm (as for example in a concentric cavity with R = 10 cm), we calculate the mode area for Nd:YAG to be approximately 4 x the mode area for NPP. The mode area may be calculated from

$$\text{mode area} = \pi \left[w(\ell/2) \right]^2 = \pi w_o^2 \left[1 + \left(\frac{\lambda(\ell/2)}{\pi w_o^2} \right)^2 \right].$$

Thus, the Nd:YAG advantage in lifetime and cross section is offset by the requirement for a larger mode area. The colinear pumping thresholds should be similar with NPP holding an edge considering that L_o will probably be less for the considerably shorter NPP laser. Further, the Nd:YAG length is fixed at approximately 1 cm, while the NPP length is adjustable depending on Nd concentration. We will see in the following calculations that NPP is clearly a better choice for miniature laser applications as far as threshold and efficiency are concerned.

b. Colinear Monochromatic Pumping Thresholds

In the following discussion, the lengths of the laser media are optimized to α_p^{-1} and η_p is assumed to be ≈ 1. For optical pumping with GaAlAs LED's, $[\alpha_p(810 \text{ nm})]$ YAG = 1.1 cm^{-1} and $[\alpha_p(799 \text{ nm})]$ NPP = 32.4 cm^{-1}. Using

$P_{th} = I_{th}$ x (mode area on laser rod face), we can calculate the incident threshold power as a function of nonresonant round trip loss. This is shown in Figure 11. We note that for all levels of reasonable output coupling NPP has a lower threshold and results in a much smaller device.

For colinear GaAlAs injection laser pumping, we find

$[\alpha_p(810 \text{ nm})]$ YAG = 3.2 cm^{-1} and $[\alpha_p(799 \text{ nm})]$ NPP = 135 cm^{-1}. In this case the increased absorption of Nd:YAG, due to the narrow bandwidth of the diode laser pump, results in a shorter Nd:YAG laser. The mode areas of the NPP laser and the Nd:YAG laser are now nearly equal. The Nd:YAG device has a lower threshold for any value of non-resonant loss (see Figure 12). The Nd:YAG laser is of reasonably small size, thus, we believe for this type of pumping Nd:YAG is a better choice.

c. Transverse Monochromatic Pumping Thresholds

In these cases we calculated I_{th} for each material optimizing $d = \alpha_p^{-1}$. However, the device size using this optimization does not result in a miniature laser for Nd:YAG (0.9 cm) but does for NPP (0.3 mm). Further, to obtain near equal thresholds for comparison purposes, the gain lengths for Nd:YAG were set equal to 1 cm, and those of NPP were set equal to 1 mm. The results are shown in Figure 13. NPP is clearly a better choice for a low threshold transversely pumped miniature laser device.

Figure 11.   Incident threshold power as a function of
non-resonant round trip loss for colinearly
LED pumped NPP and Nd:YAG mini-lasers.
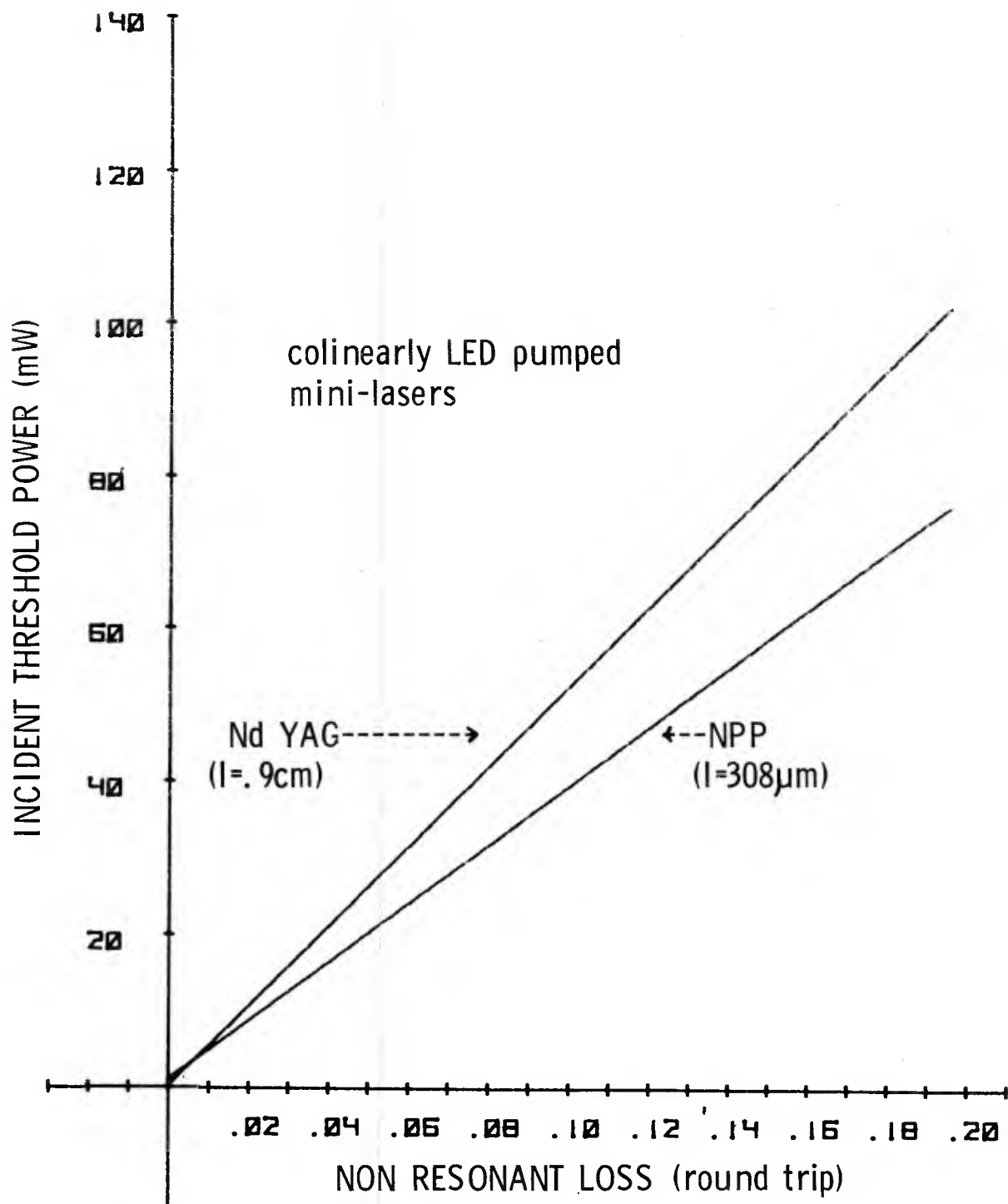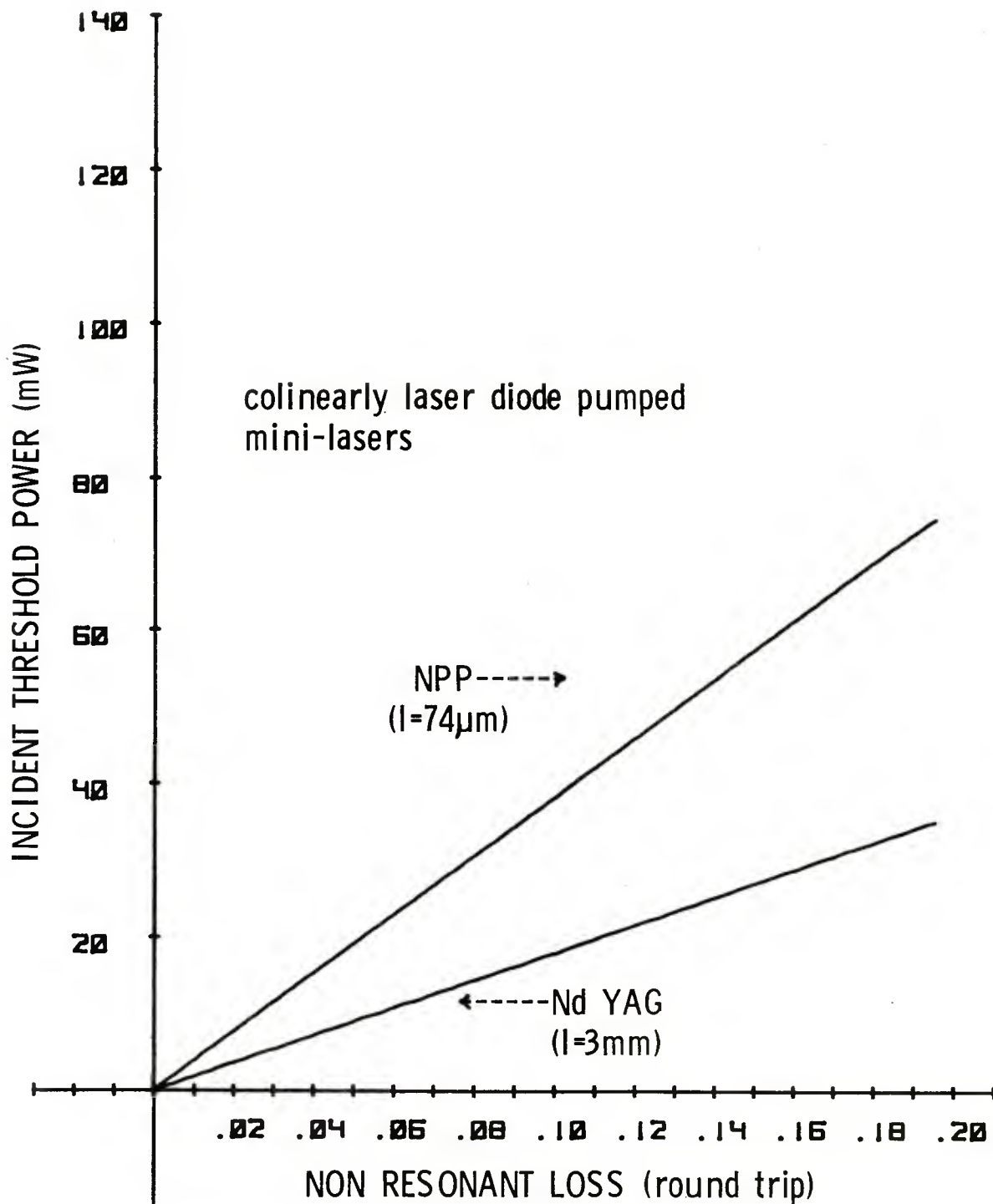
Figure 12.   Incident threshold power as a function of
             non-resonant round trip loss for colinearly
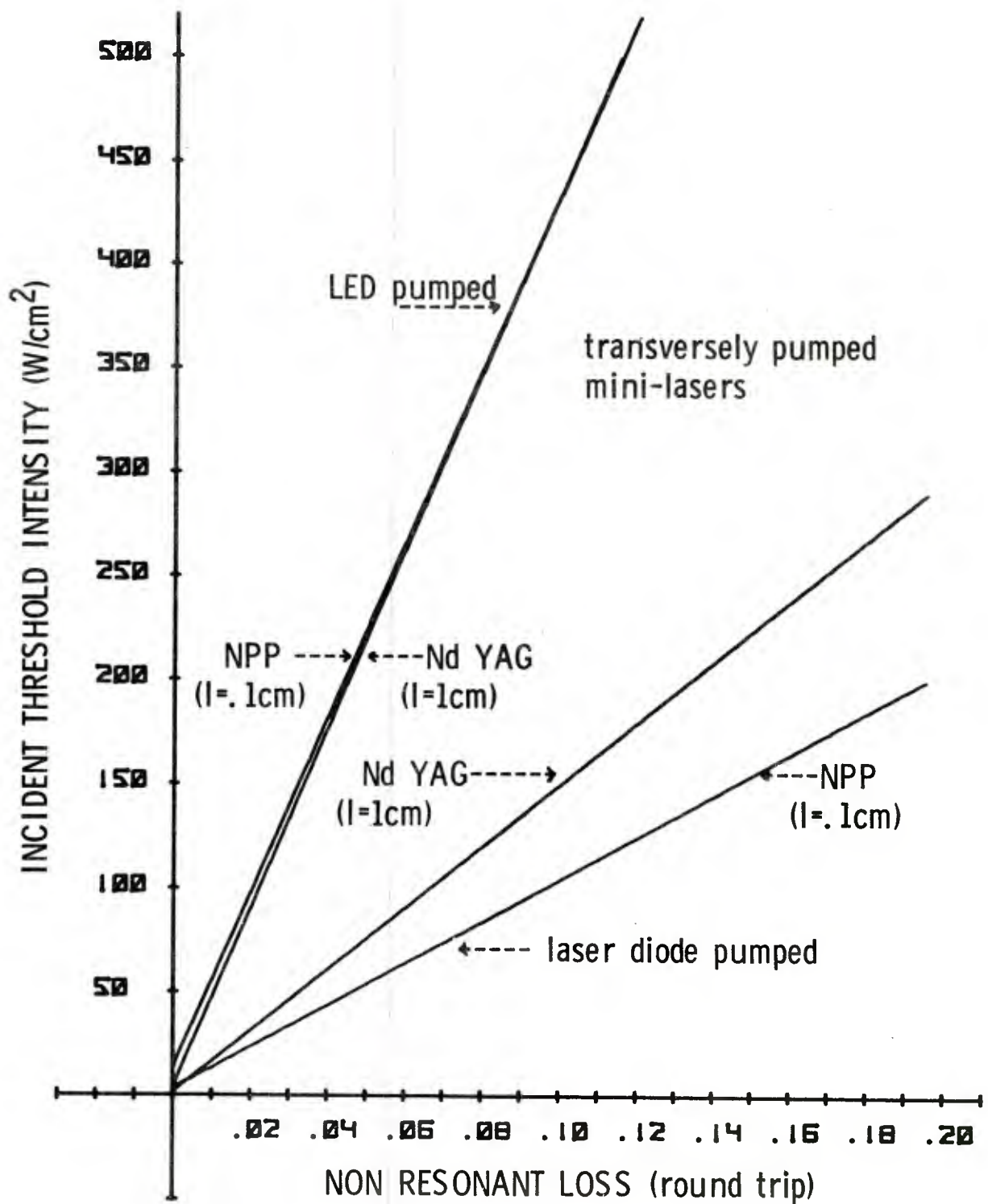   laser diode pumped NPP and Nd:YAG mini-lasers.

34

Figure 13.   Incident threshold intensity as a function of
non-resonant round trip loss for transversely
pumped NPP and Nd:YAG mini-lasers.

d. Power Output and Optimum Coupling

This section is included mainly to identify the symbols used in this report. The following analysis may be found in many standard textbooks.[19,20]

In a laser cavity containing n_i initial state ions having a decay time τ_f, the total rate of fluorescence power is

$$P_{fl} = \frac{n_i h \nu_L}{\tau_f} \quad , \quad \frac{n_i}{V} = N_i$$

the laser output power is then

$$P_{out} = (n_i - n_{th}) \frac{h \nu_L}{\tau_f}$$

since

$$n_i = \frac{P_p \tau_f n_p}{h \nu_p} \quad \text{and} \quad n_{th} = \frac{V[L]}{2 \gamma l}$$

then

$$P_{out} = (P_p - P[L]) n_p \frac{\nu_L}{\nu_p}$$

since the available laser power is the fraction of output power lost through transmission.

$$P(\text{avail}) = P_{out}(L_T/L) \text{ or}$$

$$P(\text{avail}) = (P_p [L_T/L] - P[L_T]) \frac{\nu_L}{\nu_p} \eta_p$$

19.   Lasers Light Amplifiers and Oscillators, Dieter Ross, Academic Press, London and New York (1969) p.251.

20.   An Introduction to Lasers and Masers, A. Siegman, McGraw Hill Book Co., NY (1971), p 431.

36

Setting $\frac{\partial}{\partial L_T}$ (P (avail)) = 0, the optimum transmission is found
to be

$$\left[\, L_T \,\right]_{opt.} = \left[\, L_0 + L_R \,\right]\left[\, \left(\frac{P_p}{P(L_0 + L_R)}\right)^{1/2} - 1 \,\right]$$

The maximum available power with optimized output coupling is
then

$$P(\text{max avail}) = \left[\, (P_p)^{1/2} - (P(L_0 + L_R))^{1/2} \,\right] \frac{\lambda_p}{\lambda_L} \eta_p$$

where $P(L_0 + L_R)$ is the threshold power for $L_T = 0$.

For $P_p \gg P(L_0 + L_R)$ and $\eta_p = 1$, the maximum efficiency is

$$\frac{P(\text{max. avail.})}{P_p} \approx \frac{\lambda_p}{\lambda_L} \, .$$

e. CW Laser Considerations for NPP Transversely Pumped
by a GaAlAs Diode Array

We begin with a consideration of the geometry of the diode
array. Referring to Figure 14(a), the separation between light
emitting regions is d_s, the light emitting length is d_ℓ. The
beam divergence perpendicular to the junction plane is
$\theta = 27.5^o$ (half angle to 50% points) and $\emptyset = 2.5^o$. Typically,
$d_\ell = 1$ mil = 25 μm and $d_s = 9$ mil = 229 μm. Each diode
illuminates an area on the laser rod of width $d_w = 2\,h\,\tan\theta$,
where h is the diode to rod distance. If d is the depth of the
rod, then the average gain length (at a depth d/2) is
$g_{av} = d_\ell + 2\,(h + d/2)\tan\emptyset$ (see Figure 14(b)). The total gain
length of the square cross section rod is

$$G = D\left[\, d_\ell + 2\,(h + d/2)\,\tan\emptyset \,\right]$$

37

Fig. 14(a).   GaAlAs diode array spacing d_s and light
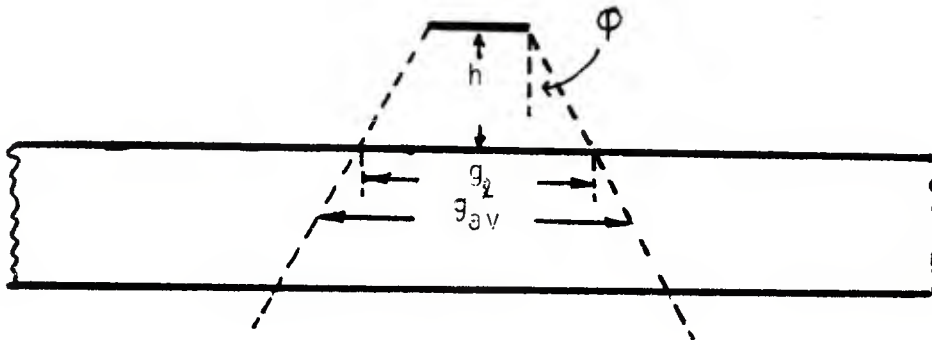emitting length d_1.

Fig. 14(b).   Illumination geometry of one of the diodes
in the array (shown above the laser rod).
Rod to diode spacing is h, g_1 is the gain
length on the rod face and g_{av} is the gain
length at a depth d/2, d is the rod length.

where D = number of diodes in the array. The equation for the power threshold for transverse pumping is

$$P_{th} = \frac{V h \nu_p [L]}{2 \gamma \tau_f G (1 - exp(-\alpha_p d))} .$$

V is the pumped volume, which is the sum of the volumes of the pyramidal pumped sections. Each pumped section is the frustrum of a pyramid of volume

$$V = d/3 [A_1 + A_2 + (A_1 A_2)^{1/2}]$$

where A_1 = area of the top and A_2 = area of the bottom.

$$A_1 = d_w (d_\ell + 2h \tan \emptyset),$$

$$A_2 = (2(d + h) \tan \theta)(d_\ell + 2 (d_w + h) \tan \emptyset).$$

the thickness d should be fabricated to be $[\alpha_p (799 nm)]^{-1}_{NPP} \approx 80 \mu m$

We arbitrarily choose h to be 25 μm. Then

$$d_w = 26 \mu m,$$

$$A_1 = 7 \times 10^{-6} cm^2$$

$$A_2 = 3.2 \times 10^{-5} cm^2$$

$$v = 1.44 \times 10^{-7} cm^3 = V/D$$

$$G = 2.8 \times 10^{-3} D cm$$

Using these values we can calculate the incident power required to reach threshold.

$$P_{th} = (0.7 (L_o + L_T) + (5.6 \times 10^{-5}) D + 5.13 \times 10^{-4} (D-1)) W.$$

39

If we arbitrarily choose a laser rod length = 1 mm, the number of diodes in the array should be equal to 5. Then $P_{TH} = (0.7 (L_O + L_T) + 2.3 \times 10^{-3})$ watts. L_O is estimated to be 0.002 and L_R is calculated to be 0.0032. Thus, $P(L_O + L_R) = 2.3$ mW and $P(max\ avail) = 0.76 ((P_p)^{\frac{1}{2}} - (2.3\ mW)^{\frac{1}{2}})$. If we use CW GaAlAs laser diodes which produce approximately 10 mW each, we have approximately 50 mW of incident power available for pumping. Applying a high reflectance coating to the opposite side of the laser rod would increase the absorption from 63% to approximately 86%. Then, the absorbed power $P_p = (1-\exp(-\alpha_p d)) P_{inc}$, where $\alpha_p = 2/d$. The absorbed power would then be 43 mW and the maximum available power would be 19.3 mW. The efficiency $P(max\ avail)/P_{inc} \times 100 = 39\%$. Assuming a 5% diode efficiency and a 100% optical transfer efficiency, an overall efficiency of approximately 2% results.

$$(L_T)_{opt} = (L_O + L_R)((P_p/P(L_O + L_R))^{\frac{1}{2}} - 1) = 0.017$$

and $R_1 R_2 = \exp(-0.017) = 0.983$. These results are plotted in Figure 15.

f. Broadband Pumping

We cannot easily calculate performance factors to obtain an indication of the response of NPP under flashlamp pumping. These calculations have been attempted in the past and recently NPP was compared to Nd:YAG.[21] NPP turns out to be an overwhelming favorite. To obtain an idea of the efficiency under flashlamp pumping, we can make the following assumptions:

η_C = conversion efficiency of electrical power to light output in the Nd pump bands = 10%.

η_T = transfer efficiency lamp to laser rod = 80%.

η_Q = quantum efficiency (average) of absorbed light to laser light = 60%.

η_A = absorbed fraction of incident pump light.

21. S. Chinn, M. I. T. Lincoln Lab., PO Box 73, Lexington, Mass., 02173, Private Communication.
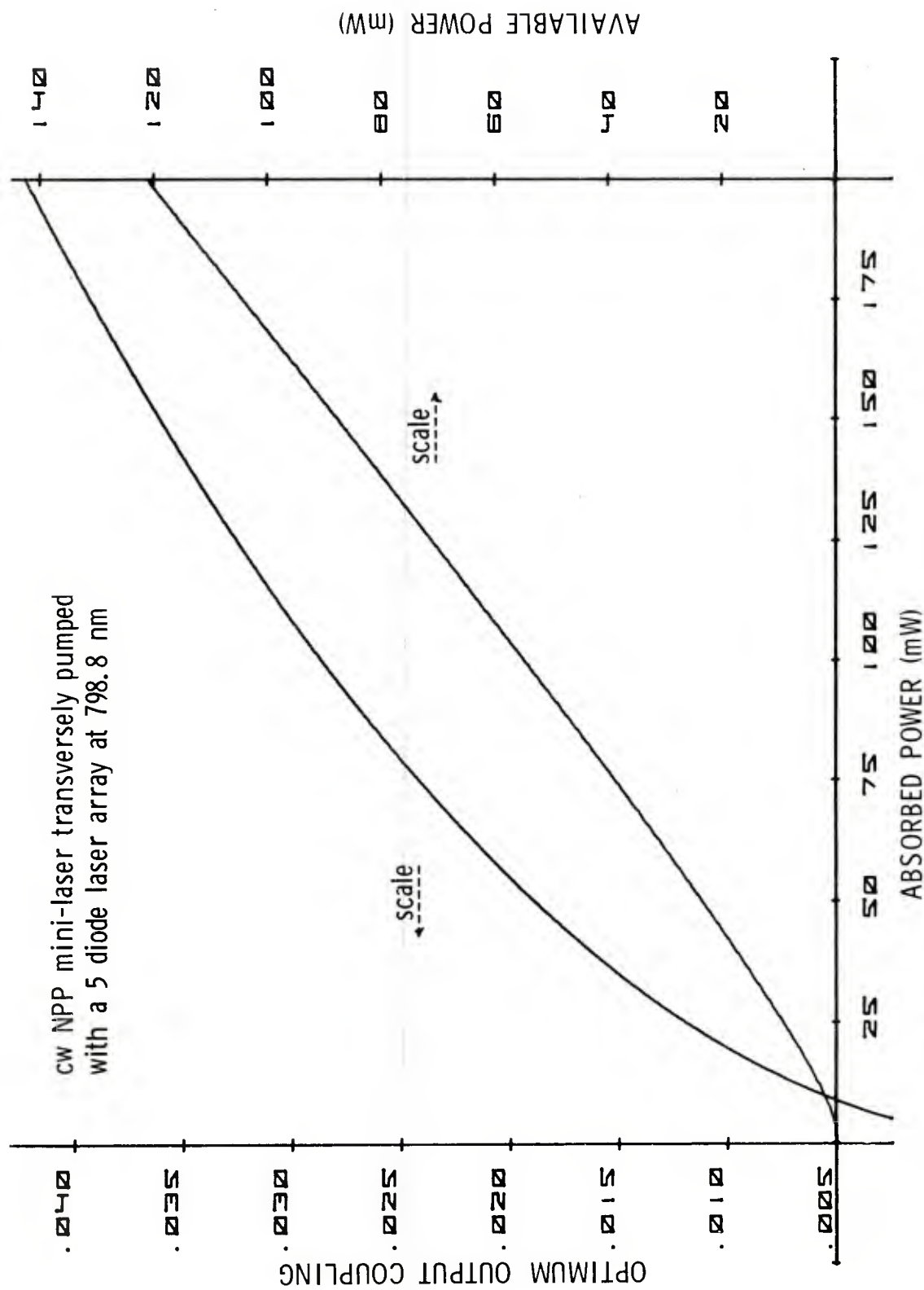
Figure 15.   Optimum output coupling and available power as a function of absorbed power for a CW NPP mini-laser transversely pumped with a 5 diode array at 798.8 nm.

41

The efficiencies η_c, η_T and η_Q are roughly equal for Nd laser
materials. However, η_A is subject to wide variation depending
on absorption coefficient and absorption length. For example,
for applications requiring 3 mm diameter lasers $\eta_A = 28\%$ for
Nd:YAG. This single pass value is found by using the effective
pump absorption coefficient α_p for pump radiation having a full-
width at half-maximum of 30 nm in the strongest pump band at
810 nm.[22] $\bar{\alpha}_p$ must be averaged over all the effective pump bands
at Nd. For 1 mm diameter Nd:YAG lasers, the strongest pump
band has an $\eta_A = 10.4\%$. NPP lasers of either 1 or 3 mm diameter
have $\eta_A > 96\%$ in the strongest pump band at 799 nm. The point
here is that even though radiation in the 30 nm band centered at
799 nm is almost completely absorbed in a single pass in NPP,
radiation in the wings of this pump band and in other weaker bands
penetrates deeper into the material. The result is that NPP
is much more efficiently pumped than Nd doped lasers. Thus,
from the laser thresholds predicted under monochromatic pumping
and the increased overall efficiency, we reasoned that NPP should
be developed as a flashlamp pumped miniature laser for low energy
applications.

DEVICE CONSIDERATIONS

    a. Potential of NPP for Use as a Fiber Optics Source for
Single Mode High Data Rate Transmission

    The NPP laser offers several advantages over both LED and
Injection Laser sources in long distance transmission systems:

    (1) Its emission wavelengths at 1.05 and 1.32 μm
coincide with two of the low-loss and low-dispersion regions of
silica fibers. Ultra low-loss fibers exhibiting 0.5 dB/km loss
have potential for repeater spacings exceeding 30 km. Thus,
benefits with respect to system economy, repeater reliability,
and maintainance are expected.

    (2) Its emission spectral width is narrower than
injection lasers -- meaning less material dispersion. Its
output is easily made single mode, single frequency making it
attractive for single mode fiber applications.

_____

    22. S. Singh, D. C. Miller, J. R. Potopowicz and L. Shick,
J. Appl. Phys. 46 1191 (1975).

(3) Its LED pumping source has an extremely long life. The overall life expectancy of the unit is on the order of 10^4 years.

(4) With transverse pumping, it is relatively simple to increase source brightness.

The expected performance of an NPP laser (transversely pumped is):

Wavelength	1.05 µm				1.32 µm	
Output power (mW)	1	1	10	10	1	10
Rod length (mm)	5	10	5	10	10	10
Incident Pump Intensity (W/cm^2)	28	25	70	45	15	50
LED Pump Power (mW)	80	65	200	130	45	175

High power GaAlAs LED's are now available in the 50-60 mW range. These can be compositionally tuned to emit at 800 nm for optimum pumping of NPP lasers. The spectral width of the LED's closely match that of the NPP laser. Each LED occupys about 1 mm of rod length. Pumping efficiencies are expected to be about 14%.

T. Kimura, et al[23] have experimented with guided wave electro-optic modulators having a bandwidth of 800 MHz and a half-wave voltage of 4V at 1.05 µm wavelength. They used a Ti diffused three-dimensional waveguide structure using external intensity modulation. The device had an extinction ratio of 13 dB and a 7.7 dB insertion loss.

b. Rangefinder Application

The latest results of bench testing flashlamp pumped NPP, using a dye solution Q-switch, external (large) mirrors and a 10 cm confocal laser cavity[24] are: For a 1 Joule input to a linear xenon filled flashlamp (1 mm bore and 10 mm discharge length), a 2 mJ output was obtained in a 7 ns pulse. A 2J lamp input resulted in a 4 mJ output in 7 ns.

---

23. T. Kimura, M. Saruwatari, J. Yamada, S. Uehara and T. Miyashita, Appl. Optics 17 2420 (1978).

24. S. R. Chinn and W. K. Zwicker, Appl. Phys. Lett. 31, 178 1977 and ERADCOM Tech Report in preparation.

With these encouraging results, we designed a miniature NPP laser cavity which could be incorporated into an experimental mini-rangefinder housing. The cavity is shown in Figure 16. An INVAR steel case holds a removable pump cavity, Q-switch and adjustable output mirror. The pump cavity is HP boron nitride, selected for its high thermal conductivity, low thermal expansion and relatively high reflectivity.* The boron nitride pump cavity holds the flashlamp and laser rod in a close coupled diffuse reflectance cylindrical space. The NPP laser rod has a rectangular parallelpiped shape of dimensions 2 x 2 x 10 mm. The long dimension is coincident with the c-axis of the crystal. The rod has 2 x 2 mm flat end faces polished to $\lambda/10$ at 587.6 nm. The faces are parallel to within 20 seconds of arc. A high reflectance coating on one face serves as the rear mirror. The other face is anti-reflection coated. The 2 x 10 mm (100) pump faces are rough ground and the other (010) faces are cleaved. The (100) face is cemented[†] to the BN for maximum heat removal since the (100) direction has the highest thermal conductivity[25] the (010) cleavage plane is also perpendicular to the cemented interface to insure maximum resistance to cleavage. The Q-switch is a saturable absorbing dye film[‡] mounted in an INVAR holder which is removable. The output mirror is HR coated for 97.5% or alternatively 82% reflectivity at 1052 nm. These mirrors are 3.75 mm in diameter, 3 mm thick and have a radius of curvature of 2 m.[§] The mirror is held in a screw adjustable INVAR mirror mount. The flashlamp is a miniature "L" shaped design (to shorten the laser cavity), xenon filled, discharge length 10 mm and bore diameter 1.2 mm.[⚡] The flashlamp is triggered externally. The calculated spot sizes are 274 μm at the curved mirror and 273 μm at the flat mirror. The calculated beam divergence is 1.2 mrad, and the measured beam divergence was 1.6 mrad. Output energy

---

25. S. R. Chinn and W. K. Zwicker, J. Appl. Phys. <u>49</u> 5892 (1979).

* Carborundum Company, Refractories & Electronics Division, Technical Ceramics Plant, PO Box 311, Latrobe, PA 15650.

† The (100) direction of NPP has a thermal conductivity of 0.021 W/cm°K, HP boron nitride is 0.61 W/cm°K. Aremco Products, PO Box 429, Ossining, NY 10562 manufactures high thermal conductivity adhesives. For example, ceramabond 503 (0.048 W/cm°K) and Aremco Coat 543 (1.43 W/cm°K) both are permanent adhesives. Aremco also supplies crystalbond 509 which is acetone soluble and crystal bond 555 which is water soluble.

‡ Manufactured by Eastman Kodak Co., Eastman Organic Chemicals, Rochester, NY 14650, Standard No. 15064 Optical Density at 1060 nm is 0.36 ± 0.02.

§ Supplied by Laser Optics Inc., PO Box 127, Danbury, CO 06810.

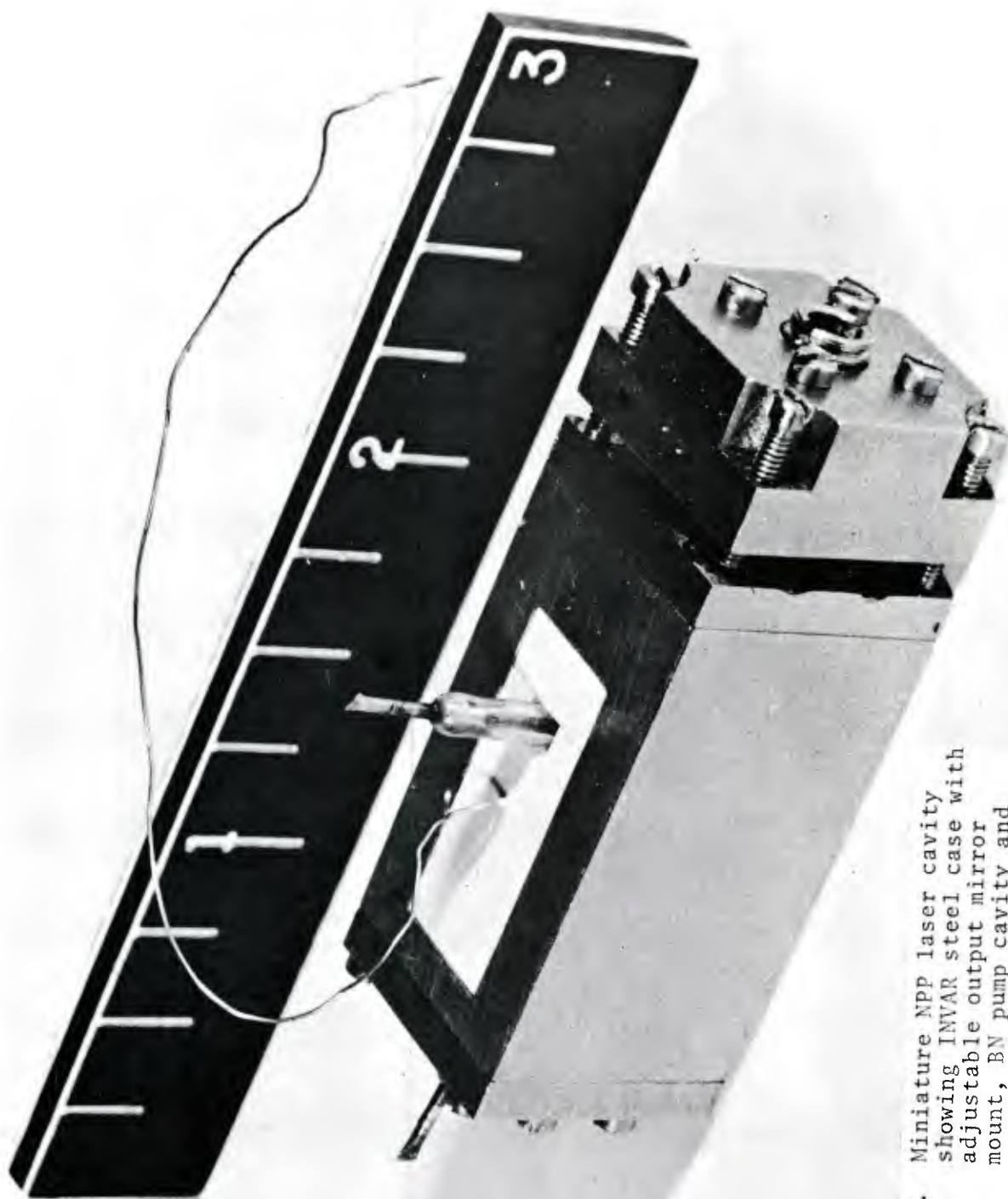⚡ Manufactured by ILC Technology, Sunnyvale, CA 94086.

Fig. 16. Miniature NPP laser cavity
showing INVAR steel case with
adjustable output mirror
mount, BN pump cavity and
L-shaped xenon flashlamp.

using a 97.5% reflectivity output mirror was 1 MJ in 60 μs. Input to the flashlamp was 400 V at 17.78 μF and 45 μH. A single-mesh discharge circuit was used and the lamp pulse duration was approximately 100 μs. Under the same conditions an 82.5% output mirror gave an energy output of 2 mJ. It, therefore, is clearly established that the pentaphosphate material is competitive material for future rangefinder developments.

SUMMARY OF ERADCOM AND ARMY/ERADCOM SPONSORED NdP_5O_{14} ACHIEVEMENTS

    a. Growth of large, perfect laser crystals (4.5 x 3 x 2.2 mm).[4]

    b. Laser output at 1.05 μm; 240 mW pulsed using an Argon laser pump (optical conversion efficiency 24%).[13]

    c. Study of the effects of crystal twinning on laser performance.[13]

    d. Unique modifications of conventional solution growth techniques yielding laser quality crystals up to 1 cm in size (patent granted).[5]

    e. Gadolinium and cerium diluted material shown to have 20% longer lifetime.[13]

    f. Calculations to show the impact of NdP_5O_{14} on future rangefinder and fiber-optic systems.[5]

    g. Technology developed for the growth of crystals up to 12 x 25 x 25 mm in size.[6].

    h. Process developed to fabricate laser rods 1 x 1 x 10 mm to 4 x 4 x 20 mm.[6]

    i. Thermal conductivity and specific heat of NPP measured and the thermally limited repetition rate estimated.[28]

    j. Operation of a miniature flashlamp pumped laser at 1.05 μm established with the following parameters: Input 1 J, Output 11 mJ in 60 μs, and 2 mJ in 7 μs.[24]

    k. New quenching model suggested based on spatial energy migration to surface quenching sites.[14]

    l. Miniaturization of NPP laser cavity, all components individually removable for easy replacement, overall size 1.5 x 1.5 x 4.4 cm.

FORECAST

    To assist future decisions on the implementation of NPP lasers for rangefinder applications, additional work is required

to increase the energy output of the miniaturized cavity. New resonator configurations will have to be designed to be accommodated in a small package. Guidelines for this effort will no doubt come from the conclusions of the Lincoln Laboratories final report. In the future, should a decision be made to cement the laser rod, dye-film Q-switch and external mirror to a common base, the overall size of the unit could be as small as 1 x 1 x 2 cm and weigh only 5 grams.

An NPP laser development program to extend the mode of operation and widen the range of applications has been suggested.[24] Specifically, a mode locked laser system would find applications in high-data-rate information transmission and in signal processing.

Future materials' development should include research to find an Nd compound laser material less susceptible to structural effects which limit the use of certain crystal directions as the laser axis.